NASA TECHNICAL NOTE

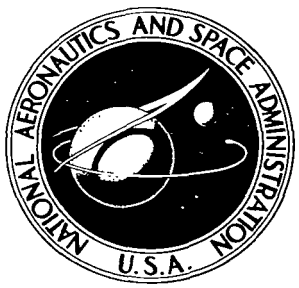

A FIXED-BASE VISUAL-SIMULATOR STUDY OF PILOT CONTROL OF ORBITAL DOCKING OF ATTITUDE-STABILIZED VEHICLES

by Donald R. Riley and William T. Suit

Langley Research Center
Langley Station, Hampton, Va.

NATIONAL AERONAUTICS AND SPACE ADMINISTRATION • WASHINGTON, D. C. • JANUARY 1964

A FIXED-BASE VISUAL-SIMULATOR STUDY OF PILOT CONTROL OF ORBITAL DOCKING OF ATTITUDE-STABILIZED VEHICLES

By Donald R. Riley and William T. Suit

Langley Research Center
Langley Station, Hampton, Va.

NATIONAL AERONAUTICS AND SPACE ADMINISTRATION

For sale by the Office of Technical Services, Department of Commerce,
Washington, D.C. 20230 -- Price $1.25

A FIXED-BASE VISUAL-SIMULATOR STUDY OF PILOT CONTROL OF ORBITAL DOCKING OF ATTITUDE-STABILIZED VEHICLES

By Donald R. Riley and William T. Suit

SUMMARY

A study has been made on a fixed-base simulator of the ability of human pilots to perform the final docking between a manned spacecraft and an orbiting tank by using only visual cues for guidance. Both vehicles were assumed attitude stabilized. The pilot was given translational control of the manned spacecraft by means of simple on-off reaction jets. The information display symbolized a docking mechanism that consisted of a square grappling bracket on the spacecraft and a spherical ball coupler on the orbiting tank. In the simulator, a painted target and a light spot projected on a cylindrical screen represented the grappling bracket and ball coupler, respectively.

The results of the investigation showed that, for most of the simulator flights, the pilots performed the docking maneuver with the following accuracies at contact:

(1) Vertical and lateral displacements of coupling mechanism of 1 inch or less

(2) Longitudinal contact velocities less than 0.1 ft/sec

(3) Residual vertical and lateral velocities of 0.04 ft/sec or less.

Flights from 40 feet to contact could be performed in about 3 minutes. The characteristic-velocity increment (an indication of fuel consumption) was small; however, it increased with an increase in control acceleration for the range investigated (0.1 to 1.0 ft/sec^2). Additional considerations herein of a human's visual capability for judging closing velocity due to size change indicate that a human pilot can serve as a sensor for information gathering with sufficient accuracy for the entire docking maneuver.

INTRODUCTION

Man's capabilities and limitations in space operations have not as yet been fully explored. It does appear, however, that man can contribute significantly to the successful accomplishment of certain mission phases. While for some mission phases he might act as an observer or in a backup capacity only, in certain other

operations man might well be utilized as the primary system. The docking phase of orbital rendezvous appears to be one operation in which man could act as the primary system for information gathering, guidance logic, and control application.

At present there exist a number of missions in space that will require the coupling together or docking of two or more vehicles. Most of the readily available literature on docking, however, is concerned primarily with automatically controlled vehicles (see refs. 1 to 5, for example). The purpose of the present paper is to present the results of a fixed-base simulator study of the ability of a pilot to perform the docking maneuvers between two vehicles, a manned spacecraft and an orbiting tank, by using only visual cues for guidance. The results provide some indication of the docking accuracies that can be expected from pilot control. Human judgment of closure rate for the docking maneuver is examined in some detail in the appendix.

SYMBOLS

d	diameter of object, ft
Δd	change in object diameter, ft
g_e	gravity at earth's surface, ft/sec^2
I_s	specific impulse, sec
k	nondimensional size-change ratio, $\Delta d/d$
m	vehicle mass, slugs
T	reaction jet thrust, lb
T/m	capsule acceleration due to thrusting, ft/sec^2
T_X, T_Y, T_Z	thrust along X, Y, and Z axes
Δt	continuous observation time for size-change determination, sec
ΔV	characteristic-velocity increment, $\left(\Delta V = g_e I_s \log_e \frac{m_o}{m_f}\right)$, ft/sec
X,Y,Z	reference axis system with origin at center of spherical ball coupler
X',Y',Z'	right-hand axis system with origin at pilot's eye in manned capsule
x,y,z	displacements of pilot's eyes along reference axis, ft
α	visual angle, deg
ω	orbital angular velocity, radians/sec

Subscripts:

f	final
min	minimum
0	initial

A dot over a symbol indicates a derivative with respect to time.

SIMULATION OF THE PHYSICAL PROBLEM

The physical problem under consideration is shown in figure 1. A symbolic docking mechanism consisting of a square grappling bracket on the manned spacecraft and a ball coupler on the orbiting tank was employed. The pilot was required to maneuver the spacecraft so as to drive the square grappling bracket over the ball coupler at a very low closing velocity. Both vehicles were assumed to be attitude stabilized. The pilot was given translational control of the spacecraft in three directions by means of simple on-off acceleration controls.

Figure 2 illustrates the visual-docking simulator that was employed to represent the physical problem. The ball target on the orbiting tank is represented by a single light spot projected on a 16-foot-diameter cylindrical screen. The position and size of the spot are controlled by an analog computer which solves the equations of relative motion between the two vehicles. The projection system consists of a cylindrical tube which contains a 25-watt point light source, a mechanized aperture that controls the size of the light spot, and a two-axis mirror that positions the light spot on the screen. The screen completely enclosed the pilot's cabin and projection system and was light tight. A small planetarium provided a star background. Since only translational motions of the vehicle are involved, the star background remained fixed. A closeup photograph of the pilot's cabin and the projection system is presented as figure 3.

The square target shown in figure 4 was painted on the cylindrical screen and represented the grappling bracket of the spacecraft. The center of the target was 8 feet from the pilot's eyes at eye level so that the line of sight to the target center was parallel to the longitudinal axis of the spacecraft.

The simulation covers the range for the physical problem from where the pilot first shifts his attention from the full-size tank and begins to concentrate on the coupling mechanism. For a 10-inch-diameter spherical ball coupler, the maximum range considered herein was about 40 feet. This value was chosen on the basis of the analysis presented in the appendix.

Only one level of spot illumination was used in the simulator tests. Light-spot luminance was estimated to be of the order of 1 foot Lambert. For the physical docking problem, the luminance of the orbiting vehicle in space can vary over a wide range which depends on whether it is under direct illumination of the sun or illuminated by reflected light from the moon or earth. References 6 and 7 provide some information on the visibility of an object in space.

EQUATIONS OF MOTION

The basic translational equations of motion of the manned spacecraft written relative to the orbiting tank are:

$$\frac{T_X}{m} = \ddot{x} + 2\omega\dot{z}$$

$$\frac{T_Y}{m} = \ddot{y} + \omega^2 y$$

$$\frac{T_Z}{m} = \ddot{z} - 2\omega\dot{x} - 3\omega^2 z$$

These equations have been used extensively in a number of rendezvous studies (for example, see refs. 8 and 9). A rotating set of axes located in the orbiting tank, as shown in figure 5(a), was employed in the derivation. Because of the range of displacements and velocities encountered during the final 40 feet of the docking phase and the fact that the pilot provides closed-loop control, the ω terms can be neglected. All of the results of the investigation presented herein were obtained by using the simpler equations.

The thrust forces T_X, T_Y, and T_Z are applied to the manned spacecraft in the directions of the reference axes which are located in the orbiting tank. Since the spacecraft and tank are assumed to be attitude stabilized and are relatively close together, the forces also act along the body axes of the spacecraft and result in a parallel alinement of axes as shown in figure 5(b).

CONTROL CHARACTERISTICS

Translational motions of the manned spacecraft were assumed to be produced by reaction jets. No time lags for these jets were considered. Spacecraft accelerations were commanded by the pilot by a three-axis finger-tip control which is visible in the pilot's left hand in figure 3. The controller was an on-off spring-centered device that required a deflection of the controller in the direction of the desired motion of the manned spacecraft. Construction of the device permitted acceleration commands to be applied along each of the three vehicle axes individually or simultaneously. Since the controller required at least $\frac{3}{8}$-inch deflection to effect a command, a visual indication that the reaction jets were firing was supplied to the pilot by means of three dim red indicator lights (one light for each axis) arranged horizontally and located on the left side of the instrument panel just forward of and at about the level of the controller.

During the final phases of docking, small corrections to the velocity and flight path may be desirable. For on-off control, the minimum velocity change obtained depends on thrust level and the minimum time the control is held in the

firing position. The minimum time depends on the combination of the man's capability and on the design and construction of the controller. Figure 6 gives typical values of time that were obtained when the pilots were asked to apply the shortest possible input. The data are for an input along a single axis and not for combined control. The results show a range of values from a minimum of about 0.02 second to a maximum of 0.14 second; an average value would be about 0.08 second.

PILOT'S TASK AND PROCEDURE

The task given the pilot was to translate the spacecraft in such a manner as to drive the square bracket over the ball coupler (fig. 1) at a very low closing velocity by using only the visual presentation. The magnitude of the longitudinal contact velocity was not specified to be within any particular range of values, except that it should be very small but greater than zero to provide for positive coupling. Since the time to complete the task was not considered critical, no restraints on flight time were imposed on the pilots. In the simulator, the pilot applied controls to try to center the light spot inside the painted target and then to make the light spot grow to fill the square. When the light spot reached 10 inches in diameter, the flight was terminated and the computer interrogated for final-position and velocity data.

TESTS

The following four sets of initial conditions for the position and velocity of the spacecraft relative to the ball coupler were employed to obtain the data presented herein:

Initial condition	x	y	z	$\dot{x}$	$\dot{y}$	$\dot{z}$
1	25	8	8	0.1	0.1	-0.1
2	25	-8	8	-.1	.1	0
3	17	17	8	-.1	.1	-.1
4	33	17	12	0	0	0

Flights for each of the preceding initial conditions were flown with the controls adjusted to provide the same value of acceleration along all three axes. Data were obtained for control accelerations of 0.1, 0.2, 0.4, 0.6, and 1.0 ft/sec^2. One additional control combination providing acclerations of 1.0, 0.5, and 0.5 ft/sec^2 along the X-, Y-, and Z-axes, respectively, was also investigated.

RESULTS AND DISCUSSION

All the results presented herein were obtained with the authors as the pilots. A number of other subjects, including three research pilots and several engineers with simulator experience also flew the simulator. Most of these flights were made with the lower control accelerations. In general, the results obtained for most subjects were comparable (after some practice) with those presented herein.

Typical Trajectories

The trajectory of a typical flight is shown in figures 7(a) and 7(b), and the corresponding displacement and velocity time histories are given in figure 7(c). The trajectory traces of figure 7(a) are for lateral and vertical displacements plotted against longitudinal displacement. Figure 7(b) presents a projection of the trajectory in a plane normal to the pilot's line of sight through the target center. Since the figures show relative position, the trace, using the axis system depicted in the figure, represents the trajectory of the center of the spherical ball coupler relative to the pilot's eyes, and as such is representative of the trace of the light spot in the simulator.

For the physical case considered in figure 7, the ball coupler was at an initial range of about 40 feet with zero relative velocity. At this range, the light spot was about 2 inches in diameter on the screen. Initially, the pilot applied the controls successively in y and then z until a desired rate and direction of motion were obtained. Since a reduction in the y- and z-displacements reduces the range, the light spot begins to grow in size. The time histories of figure 7(c) show that before removing the vertical and lateral velocities, the pilot recognized that he could safely initiate a small closing velocity and did so. When the light spot was reasonably centered and the vertical and lateral velocities were nearly zero, the pilot increased the longitudinal closing velocity. From this point to contact, the controls and the display were conveniently uncoupled into x-control for growth-rate adjustment and y- and z-controls for centering. It is interesting to note that in the last 18 feet of travel the vertical and lateral displacements were never more than $\pm 1/2$ foot. Corresponding transverse velocities during this period were 0.03 ft/sec or less. This flight was made with the acceleration level of the controls set at 0.1 ft/sec^2 which was the lowest value used in the study.

A flight for different initial displacements and with small initial velocities is shown in figure 8. The initial range was 25 feet which corresponds to a light-spot diameter on the screen of about 3 inches. As in the previous case, the pilot initially applied the y- and z-controls to center the light spot. As the range decreased because of the reduction in y and z and the reduction in x caused by the initial velocity, the light spot grew very rapidly in size. The pilot, consequently, applied a thrust with the x-control to increase the longitudinal displacement between vehicles before the centering task could be completed. The trajectory traces of figure 8 indicate that the pilot permitted the light spot to decrease in size until the initial centering task was completed before he

reestablished a closing rate. This flight is interesting in that the pilot apparently decided, on the basis of the rapid growth of the light spot and from its size in relation to the target, that he had insufficient time to center the light spot and to reduce the transverse velocities to zero before contact. Reducing $\dot{x}$ to zero would have been sufficient to permit completion of the initial centering task, however the light spot would have continued to grow in size because of the reduction in y and z. To judge the contributions to size and growth rate from the vertical, lateral, and longitudinal components with only the visual presentation would be difficult. Apparently the pilot, to assure himself of positive control, preferred to see the light-spot diameter shrinking slowly until the initial centering was complete. Once the closing rate was reestablished, the transverse displacements up to contact were always less than $\pm 1/2$ foot. This result is similar to that of the preceding flight and was characteristic of most of the simulator flights of this investigation.

Some indication of the effect of control acceleration is presented in figure 9 where the trajectory traces are given for two flights having different initial conditions. The trajectories, however, are shown only for the final 15 to 20 feet in longitudinal displacement before contact. The acceleration levels of the controls were 0.1 and 1.0 ft/sec^2. For the higher acceleration case, figure 9 shows that the vehicles were pushed apart just prior to contact to permit the pilot to obtain better centering. A comparison of the x-y trajectory traces for the two cases indicates a more erratic path for the higher acceleration. This would be expected from an acceleration-command control system. The increased difficulty in the centering task just prior to contact was particularly noticeable during these tests. The pilot's preference for control acceleration was 0.1 or 0.2 ft/sec^2 because they believed they had better control near contact. In general, the quantitative results of this investigation show little effect of control-acceleration level. This result would indicate that although the pilots were working harder at the centering task as acceleration level increased, no degradations in pilot performance occurred in the acceleration range of this investigation.

Position at Contact

Figure 10 presents the center portion of the square grappling bracket with the crosshair representing the center. Each of the 50 data points represents the center of the light spot at the completion of a flight. All the data fell within a $2\frac{1}{2}$-inch square with the majority inside a 1-inch square. An examination of the data shows no apparent effect of control acceleration for the range investigated. Acceptable limits on the centering task at contact were not specified to the pilots during these tests. In flying the simulator it soon became apparent that perfect centering was almost an impossibility. A feeling developed, however, that the final position for a successful flight would be within an inch of the target center.

In a number of instances when the controls were set for an acceleration of 1.0 ft/sec^2, the pilot was satisfied to accept some transverse displacement at contact even when a sufficient longitudinal displacement existed between vehicles

to permit a centering correction. This condition existed only because the light spot was highly sensitive to control near contact and the pilots believed that an attempt to improve the situation might only succeed in making it worse. Although the transverse sensitivity of the light spot to control inputs increases as the vehicles draw closer together, irrespective of the level of control acceleration, the sensitivity with a setting of 1.0 ft/sec^2 was such that the pilots were essentially flying the residual motion between two opposite control inputs – that is, for close centering, the pilot would apply a nearly minimum control along one axis and then immediately apply a nearly minimum opposite control. The time delay between inputs permitted a transverse displacement of the light spot to occur. The difference in magnitude between these two inputs provided residual motion of the light spot smaller than that possible with a minimum control input. This residual motion along with the position of the light spot relative to the target center would determine when the next correction would be attempted. The fact that the pilots were successful in performing the task under these conditions is evidenced by the displacements shown in figure 10. This technique was not found necessary when the lower values of control acceleration were employed.

Velocity at Contact

The longitudinal and transverse velocities existing at contact are presented in figure 11 for 50 individual flights. The results were obtained by two pilots using four sets of initial conditions at each acceleration level. The magnitude of the longitudinal contact velocity was not specified for the pilots, except that it should exist for positive coupling and be near zero. The data in figure 11(a) indicate values of $\dot{x}$ between a minimum of 0.014 ft/sec and a maximum of 0.170 ft/sec. No effect of control-acceleration level is evident in the data. Although the values shown for a value of $T/m = 1.0$ in the x-, y-, and z-controls are lower than for the special case where $T/m = 0.5$ in the transverse controls, the docking task was considerably easier for the latter condition because of the lower sensitivity of the transverse controls. The results show that the longitudinal contact velocity for 96 percent of the flights was below 0.12 ft/sec and that for 50 percent of the flights values were below 0.06 ft/sec. In general these results indicate that the pilots could consistently establish a low closing velocity with a simple judgment on growth rate. The presence of the target was of some assistance in establishing these low values. Not only did it define the end conditions but its presence enabled the pilot to make comparisons with a reference for rate determination. An analysis of a human's minimum visual capability to detect size change contained in the appendix indicates that even without the use of a target, contact velocities of these magnitudes can be expected from pilot control.

Figure 11(b) presents the corresponding transverse velocity components at contact. In general the magnitude of these velocity components was much lower than the longitudinal velocity component. Most of the data points were below 0.02 ft/sec. These results are commensurate with the close centering task required of the pilots.

Fuel Consumption

An indication of the fuel consumed for the docking maneuver is shown in figure 12 for one specific set of initial conditions. The results are in the form of a total thrusting time plotted against flight time. This total thrusting time was obtained by summing the control-on times for all three axes. The various symbols correspond to flights with different acceleration levels of the controls. The solid curves represent theoretical minimum curves for the different acceleration levels. These were obtained by computing the thrusting time required to reduce simultaneously the x-, y-, and z-displacements between the grappling bracket and ball coupler to zero in the given flight time. Zero relative velocity between couplers at contact was also imposed as an end condition for the calculations.

The results in figure 12 are presented in the form of a characteristic velocity ΔV plotted against flight time in figure 13. The values of ΔV were obtained by multiplying the total thrusting time of figure 12 by the acceleration level of the controls. The data show that the pilot is using from 3 to 10 times the minimum fuel to perform the task. It should be noted however that the ΔV used is a small number and consequently the magnitude of this ratio is not too significant.

The effect of control acceleration on fuel consumption is illustrated in figure 13 for one set of initial conditions and in figure 14 for the four different sets of initial conditions used in this study. The results indicate that as acceleration level is increased there is a tendency for the fuel consumption to increase. This increased fuel consumption is believed to be due to the increased difficulty in the centering task during the last 10 to 15 feet of the maneuver with increasing control acceleration. It is interesting to note that the increase in ΔV with control acceleration was the only measured effect of acceleration level for the docking maneuver.

Flight Time

The data shown in figures 12 and 13 indicate that for this one particular set of initial conditions, flight times from $1\frac{1}{4}$ minutes to $5\frac{1}{4}$ minutes were utilized. Flight times for the remainder of the data were within this range. The reason for long flight times in relation to the small initial displacements between vehicles is considered to be due to the fact that no sense of urgency for task completion was imposed on the pilots. Some data not presented herein indicate that pilots could perform the assigned task in less time when asked to do so. Under these conditions, a maximum flight time of about 3 minutes could be expected for accomplishment of the task.

SUPPLEMENTAL TESTS

Since low closing velocities are required for docking, a number of additional tests were made to obtain some measure of the minimum longitudinal velocity that

might be expected from pilot control. These tests were made along only the X-axis. Elimination of the centering task permitted the pilot to concentrate only on a single variable, that of size change of the light spot. For these tests the star background was retained; however, the square grappling target that was painted on the screen was removed since not all docking configurations being considered would supply such a convenient measuring unit. Initial conditions included both closing and receding velocities with the vehicles positioned various distances apart. The pilot's instructions were simply to stop the relative motion between the vehicles within a reasonable time. When the pilot felt he had fulfilled the task, the problem was stopped and the computer was interrogated for final position and residual velocity.

The final positions of the vehicles at termination of the problem depended, of course, on the position and velocity at the initiation of the problem. Since the pilot was not required to judge range or to position at a given range but only to arrest the relative motion, the final longitudinal displacements of the spherical ball coupler varied from a range of about $5\frac{1}{2}$ feet to 42 feet for all of the data taken. Of particular interest are the values that were obtained in the vicinity of the grappling bracket location which was 8 feet from the pilot's eyes. This portion of the data is presented in the following table. The acceleration level of the longitudinal control was set at 0.1 ft/sec^2 for these tests. The final observation time Δt_f is the time from last control input to termination of the problem.

Pilot A			Pilot B		
x, ft	$\dot{x}$, ft/sec	Δt_f, sec	x, ft	$\dot{x}$, ft/sec	Δt_f, sec
10.2	0.009	10.7	8.0	0.001	25.0
7.3	0.003	5.4	11.1	0.005	12.0
8.4	-0.006	10.5	9.4	-0.002	6.5
5.9	0.005	10.5	10.3	-0.01	29.0

The results of the tests indicate that the magnitudes of the residual velocities were 0.01 ft/sec or less. For the observation times used, the corresponding velocity results were below the threshold for a human to detect a visual change in light-spot size as derived in the appendix. The results illustrate that, at least for a single task, a pilot could provide simple guidance as to how long to apply thrust, when to apply it, and perform the actual application to within his visual capabilities as an information sensor.

CONCLUDING REMARKS

A study has been made on a fixed-base simulator of the ability of human pilots to perform the final docking between a manned spacecraft and an orbiting tank by using only visual cues for guidance. Both vehicles were assumed attitude stabilized. The pilot was given translational control of the manned spacecraft by means of simple on-off reaction jets. The information display symbolized a docking mechanism that consisted of a square grappling bracket on the spacecraft and a spherical ball coupler on the orbiting tank. In the simulator, a painted target and a light spot projected on a cylindrical screen represented the grappling bracket and ball coupler, respectively.

The results of the investigation showed that, for most of the simulator flights, the pilots performed the docking maneuver with the following accuracies at contact:

(1) Vertical and lateral displacements of coupling mechanism of 1 inch or less

(2) Longitudinal contact velocities less than 0.1 ft/sec

(3) Residual vertical and lateral velocities of 0.04 ft/sec or less.

Flights from 40 feet to contact could be performed in about 3 minutes. The characteristic velocity increment (an indication of fuel consumption) was small; however, it increased with an increase in control acceleration for the range investigated (0.1 to 1.0 ft/sec^2). Additional considerations of a human's visual capability for judging closing velocity due to size change indicate that a human pilot can serve as a sensor for information gathering with sufficient accuracy for the entire docking maneuver.

Langley Research Center,
National Aeronautics and Space Administration,
Langley Station, Hampton, Va., August 28, 1963.

APPENDIX

SOME CONSIDERATIONS OF MINIMUM DISCERNIBLE CLOSURE RATES OBTAINED FROM VISUAL CUES

Introduction

The docking maneuver for pilot control using visual cues can be considered to begin when the pilot's vision includes an input from the apparent change in size of the orbiting vehicle. For vehicles of conventional size with diameters of 5, 10, and 20 feet or larger and reasonable closing velocities, initial displacements of hundreds of feet can be involved. Successful docking performance from these ranges up to the point of contact depends a great deal on the ability of a pilot to interpret visual size changes as vehicle closing velocities. The pilot must be able to make these judgments in order to take appropriate control action. An evaluation of a human's ability to interpret size change as vehicle closing velocity is, therefore, of considerable interest. Of particular concern is the minimum discernible closing velocity since this defines the slowest vehicle closure rates that can be obtained from pilot control. An approximate expression for a human's complex visual ability in this regard is derived and discussed in the following sections of this paper.

Mathematical Development

Human judgment of displacement of a two-dimensional object of known size is a function of the visual angle. The geometric relationship between visual angle, object size, and displacement is illustrated by the following sketch and given by equation (A1).

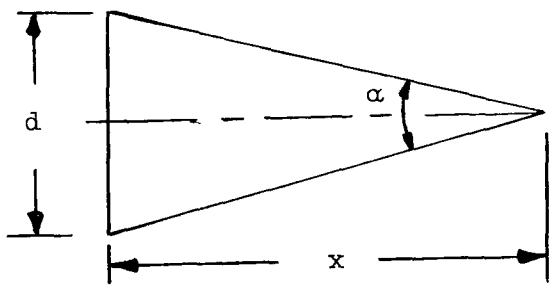

$$\alpha = 2 \tan^{-1} \frac{d}{2x} \qquad \text{(A1)}$$

Differentiation of equation (A1) with respect to time for an object of fixed size yields:

$$\dot{\alpha} = -2\left[\frac{(d/2x)}{1 + (d/2x)^2}\right]\frac{\dot{x}}{x} \tag{A2}$$

Equation (A2) provides the geometric relationship between the time rate of change of visual angle and the velocity and displacement of the object. Equation (A2) can also be used to determine minimum discernible closing velocity x_{min} for an object of fixed size as a function of x. To do this requires the use of the corresponding value $\dot{\alpha}_{min}$ in equation A-2, where $\dot{\alpha}_{min}$ must be evaluated in terms of human visual capability.

It is anticipated that during the final docking phase the closing velocities will be low. The feeling of closure will come principally from a change in the apparent size of the object in the pilot's visual field which suggests the following way of evaluating $\dot{\alpha}_{min}$.

Consider equation (A1) and the associated sketch. If x is assumed to be constant and object size d is allowed to vary, a corresponding change occurs in α. Taking a time derivative of equation (A1) and holding x constant yields

$$\dot{\alpha} = 2\left[\frac{(d/2x)}{1 + (d/2x)^2}\right]\frac{\dot{d}}{d} \tag{A3}$$

now let

$$\dot{d} = \frac{\Delta d}{\Delta t}$$

upon substitution

$$\dot{\alpha} = 2\left[\frac{d/2x}{1 + (d/2x)^2}\right]\frac{\Delta d}{\Delta t d} \tag{A4}$$

Now $\frac{\Delta d}{d}$ may be recognized as the form of a Weber Ratio (refs. 10 and 11). Since $\dot{\alpha}_{min}$ is desired from equation (A4) Weber's law can be applied. This law states that the minimum change in stimulus intensity which can be perceived divided by the intensity of the original stimulus is a constant.

$$\frac{\Delta d}{d} = k \tag{A5}$$

where

d intensity of a stimulus (light-spot diameter)

Δd minimum change in stimulus intensity that human perception can acknowledge as a change (minimum perceptible change in light-spot diameter)

k constant

Weber's law has been applied to measurements in vision and hearing and has been found to be valid for a wide range of stimulus intensities. It is known to be unreliable only at very low or extremely high stimulus intensities.

Equation (A4) can now be rewritten as

$$\dot{\alpha}_{min} = 2\left[\frac{d/2x}{1 + (d/2x)^2}\right]\frac{k}{\Delta t} \tag{A6}$$

The Δt appearing in equations (A4) and (A6) is the time increment during which the change in stimulus occurred and consequently is the observation time. For the docking of two objects, large values of Δt - greater than 30 seconds, for instance - would be unrealistic in that it would be difficult for the pilot to tell if a change in stimulus approaching the minimum had occurred. Time increments from 5 to 15 or 20 seconds would seem to be the practical range for observation time.

Upon substitution of equation (A6) for $\dot{\alpha}$ into equation (A2) there results

$$\frac{\dot{x}_{min}}{x} = -\frac{k}{\Delta t} \tag{A7}$$

Equation (A7) provides an expression for the minimum discernible closing velocity and indicates that $\dot{x}_{min}$ is proportional to the displacement and inversely proportional to the observation time. For a positive value of k, the negative sign in equation (A7) indicates that $\dot{x}_{min}$ is a closing velocity.

Evaluation of k

To establish a realistic value of k (the percent size change necessary for detection), a portion of the results of the tests along a single axis presented in the section entitled "Supplemental Tests" was employed. The time from the initiation of the problem until the first control input occurred is plotted against initial values of $x/\dot{x}$ in figure 15. According to equation (A7), k should be the slope of this curve. Since the pilots were asked to reduce the relative velocity to zero in a reasonably short time period but with no time limit imposed, the results could be expected to scatter. A lower boundary should exist, however, which would define k. The curve shown is for $k = 0.05$. Since the data used in figure 15 were obtained for several discrete initial displacements, the data can be conveniently plotted as a function of $\dot{x}$. These results are shown in figure 16. The data indicate that for most of the flights, the pilots did not permit too long a time to elapse beyond the minimum before initiating a control input.

A situation somewhat similar to that occurring at the beginning of a flight also exists at the end of a flight. If the curve for $k = 0.05$ in figures 15 and 16 is a lower boundary for the time from problem initiation to the first control input, then it seems reasonable that it should also be the upper boundary for the time from the last control input to the end of the run. That is, the time to

first control input must be equal to or greater than the boundary since the boundary is a minimum discernible one. At the completion of a run, however, the pilot should have applied sufficient control such that after observing the results for a given observation time Δt, the corresponding value of $x/\dot{x}$ should be below the boundary. Figure 17 indicates that this is as expected.

A value of k of 0.05 is a common one used with Weber's law and has been found to apply in many situations (for example, see ref. 10). In addition, the results of a detailed study on perceived movement in depth (ref. 7) indicate that a pilot would detect a given motion 90 percent of the times he observed it if an apparent 5-percent size change occurred; observation times from 0.6 to 20 seconds were employed. Reference 7 also discusses the possibility of a k value as low as 0.02, but with a k value of 0.02 the certainty of detection was only 75 percent. The data point shown at $x/\dot{x} = 400$ in figure 15, for example, corresponds to about a 3-percent size change, and according to reference 7 the certainty of detection would be about 80 percent.

On the basis of references 7 and 10 and figures 15 and 17, a value of k of 0.05 is believed to be realistic and should provide a certainty of detection of at least 90 percent for the range of observation times being considered. This value of k can be expected to hold over a reasonable range of visual angles. Deviations from this value can be expected for both large and small visual angles. For example a rapid increase in the value of k can be expected for visual angles less than $1/2^{\circ}$ (see ref. 10). For the docking mechanism considered in the simulation, the upper limit of the visual angle on k would not be exceeded since the pilot would be expected to shift his area of concentration from the full-size tank to the coupler mechanism somewhere within the last 50 feet of vehicle separation. Some information on large visual-angle inputs to pilots for rate determination is available in reference 12.

General Discussion

Typical results for visual angle and visual-angle rate are illustrated in figures 18 and 19 for vehicle displacements less than 50 feet. The curves were constructed for the configuration in figure 1 for a tank diameter of 5 feet, and for a 10-inch-diameter coupler ball. For convenience, in the calculations for the tank, it was assumed that the distance between the ball coupler and the front of the tank was zero. Figures 18 and 19 illustrate the rapid increase in visual angle and visual-angle rate with decreasing displacement for both the tank and ball coupler. The calculations for visual-angle rate were made for an arbitrary closing velocity of 1 foot per second. Figure 19 also includes curves for minimum human visual capability as computed from equation (A6) for one observation time ($\Delta t = 5$ sec). It is interesting to note that the visual-capability curves show an increase in $\dot{\alpha}$ with increasing visual angle (decreasing range). The calculated values near contact for the tank may be in error due to the large visual angles (fig. 18) for which k may not be 5 percent. Comparisons between the physical and visual curves for either the tank or the coupler, however, show the expected rapid divergence of the curves with decreasing displacement.

It is of interest to note that equation (A7) predicts identical closing velocities for observation of either the full-size tank or the ball coupler for vehicle displacements approaching 100 feet. At ranges greater than 100 feet, observations of the full-size tank are superior for closure-rate information since the visual angle α for the ball coupler is less than $1/2^{\circ}$. Although a pilot could center his area of concentration on the coupler rather than the tank at 100 feet without a loss of visual capability, it would seem that in an actual docking maneuver he would prefer to observe the larger object at least until the visual angle of the coupler was of the order of 1° to 2°. Figure 18 indicates that the earliest observation of the coupler would be at a range of about 40 to 50 feet.

The significance of equation (A7) for determining minimum discernible closing velocity is illustrated in figures 20 and 21. Figures 20 and 21 provide a comparison of a human pilot's visual capability with translational motion characteristic of the spacecraft. Figure 20 covers the close-in phase where the separation distance between the pilot's eyes and the orbiting vehicle is 50 feet or less. Figure 21 considers relatively large displacements up to about 2,000 feet. The figures are performance charts that present closing velocity against displacement. The vehicle performance curves were computed for the docking configuration considered herein and show the maximum closing velocity at any displacement that would be reduced to zero at contact by a given thrust level if applied continuously. The calculated curves of visual capability indicate the minimum velocity at any range that can be detected consistently in the stated observation time. For example, figure 20 shows that if a pilot can observe the orbiting vehicle for 5 seconds when the displacement is 50 feet he can detect closing velocities 1/2 ft/sec or greater. Velocities less than 1/2 ft/sec would be undetected for a 5-second viewing time. Increasing observation time reduces this 1/2 ft/sec minimum. The probability of detection associated with the visual curve is believed to be at least 90 percent.

The visual curve shown in figure 21 for larger ranges has been included to illustrate the degradation in visual ability as the visual angle gets small. The curves shown are, at best, guesses based on the fact that a larger percentage size change is needed for a human to detect differences when the visual angle is small (of the order of $1/2^{\circ}$ or less). The value of k expresses the size-change relationship. The approximate curve shown in figure 21 was arbitrarily used to depict this effect and was obtained from reference 10. The results of figure 21 are illustrative only; however, they indicate that the visual curve and vehicle-performance curves cross at some relatively large separation distance. It should be noted that the visual curve in figure 20 is independent of vehicle size, at least, within some reasonable visual-angle range. Such is not the case for the larger ranges where k begins to vary with visual angle. The curves shown in figure 21 are for a 5-foot-diameter vehicle. Increasing vehicle diameter would, of course, shift the curves toward the larger values of displacement. Although admittedly approximate, the results of figure 21 give some idea of the magnitude of the maximum closing velocity that can exist at the initiation of docking. The intersections of the curves define the maximum possible values of range and range rate that can be controlled by a pilot for a visual docking maneuver.

Equation (A7) as derived herein is intended only as an approximation to a human's complex visual ability. As such, it gives some idea of the very low velocities during the final 50 to 100 feet of the docking maneuver that can be detected visually. At vehicle contact ($x = 8$ ft, for example), minimum discernible closing velocities of 0.02 to 0.08 ft/sec for corresponding observation times of 20 to 5 seconds, respectively, are obtained.

REFERENCES

1. Ward, J. W., and Williams, H. M.: Orbital Docking Dynamics. [Preprint] 1953-61, American Rocket Soc., Aug. 1961.

2. Kamm, Lawrence J.: SATRAC: Satellite Automatic Terminal Rendezvous and Coupling. [Preprint] 1497-60, American Rocket Soc., Dec. 1960.

3. Schroeder, W.: A Terminal Guidance Scheme for Docking Satellites. [Preprint] 1952-61, American Rocket Soc., Aug. 1961.

4. Fox, J. C., and Windeknecht, T. G.: Six Degree-of-Freedom Simulation of Manned Orbital Docking System. 9352.8-37, Space Tech. Labs., Inc., Apr. 1962.

5. Post, Joseph: Orbital Rendezvous Positioning Indexing and Coupling System: Automatic, Semiautomatic. Northrop Corp., Norair Division Tech. Memo. ASG-TM-61-77, 1961.

6. Martin, Dennis J.: The Visibility of an Object in a Space Environment. S.M.F. Fund No. FF-31, Inst. Aerospace Sci., Jan. 1962.

7. Baker, Charles A., and Steedman, William C.: Perceived Movement in Depth as a Function of Luminance and Velocity. Human Factors, vol. 3, no. 3, Sept. 1961, pp. 166-173.

8. Eggleston, John M., and Beck, Harold D.: A Study of the Positions and Velocities of a Space Station and Ferry Vehicle During Rendezvous and Return. NASA TR R-87, 1961.

9. Eggleston, John M.: A Study of the Optimum Velocity Change to Intercept and Rendezvous. NASA TN D-1029, 1962.

10. Epple, R. G. E.: The Human Pilot. Volume III - Fundamentals of Design of Piloted Aircraft Flight Control Systems. BuAer Rep. AE-61-4, Bur. Aero., Aug. 1954.

11. Stevens, S. S., Ed.: Handbook of Experimental Psychology. John Wiley & Sons, Inc., 1960.

12. Lina, Lindsay J., and Assadourian, Arthur: Investigation of the Visual Boundary for Immediate Perception of Vertical Rate of Descent. NASA TN D-1591, 1963.

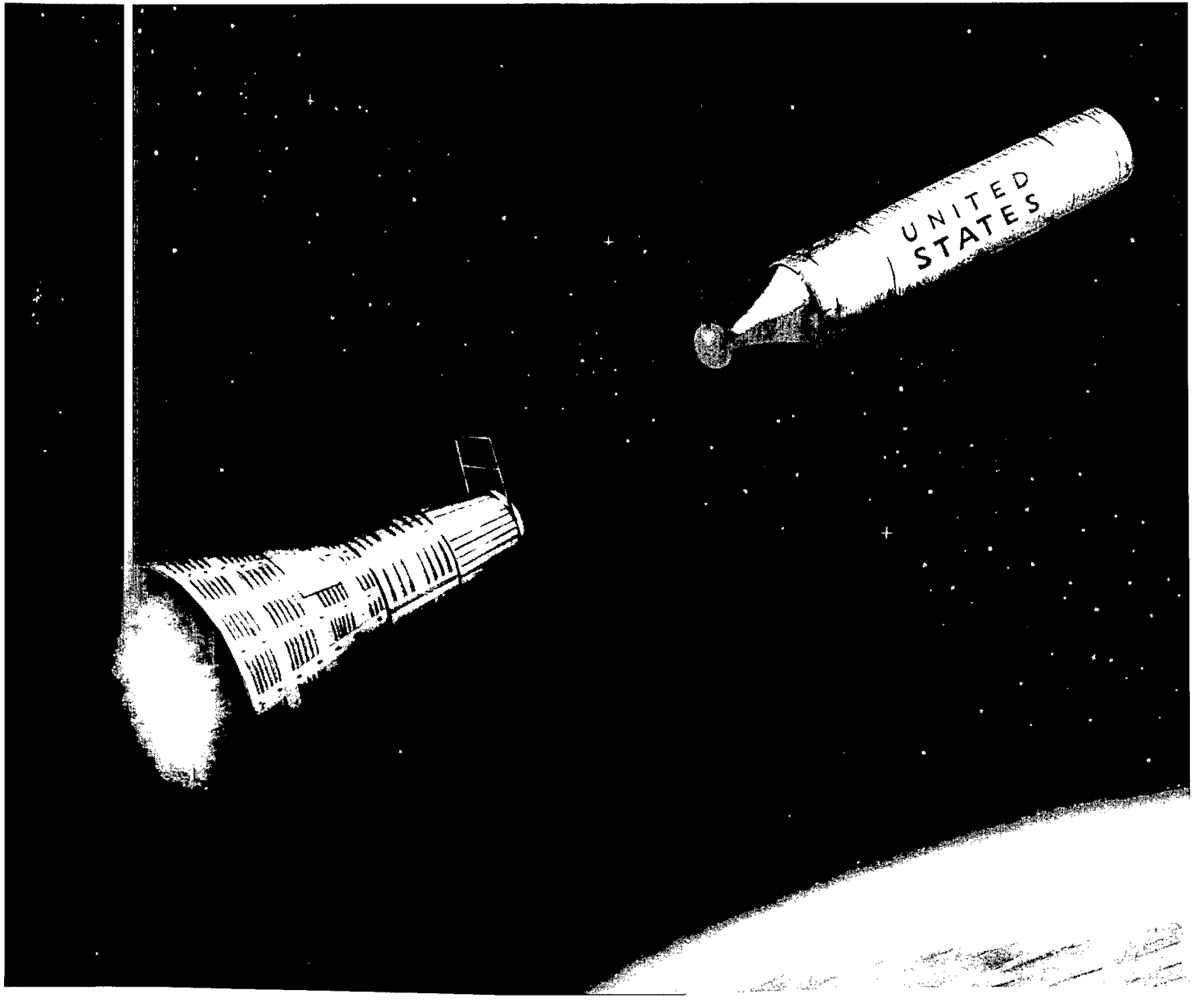

Figure 1.- Physical representation of simulation using symbolic docking mechanism. L-62-5691

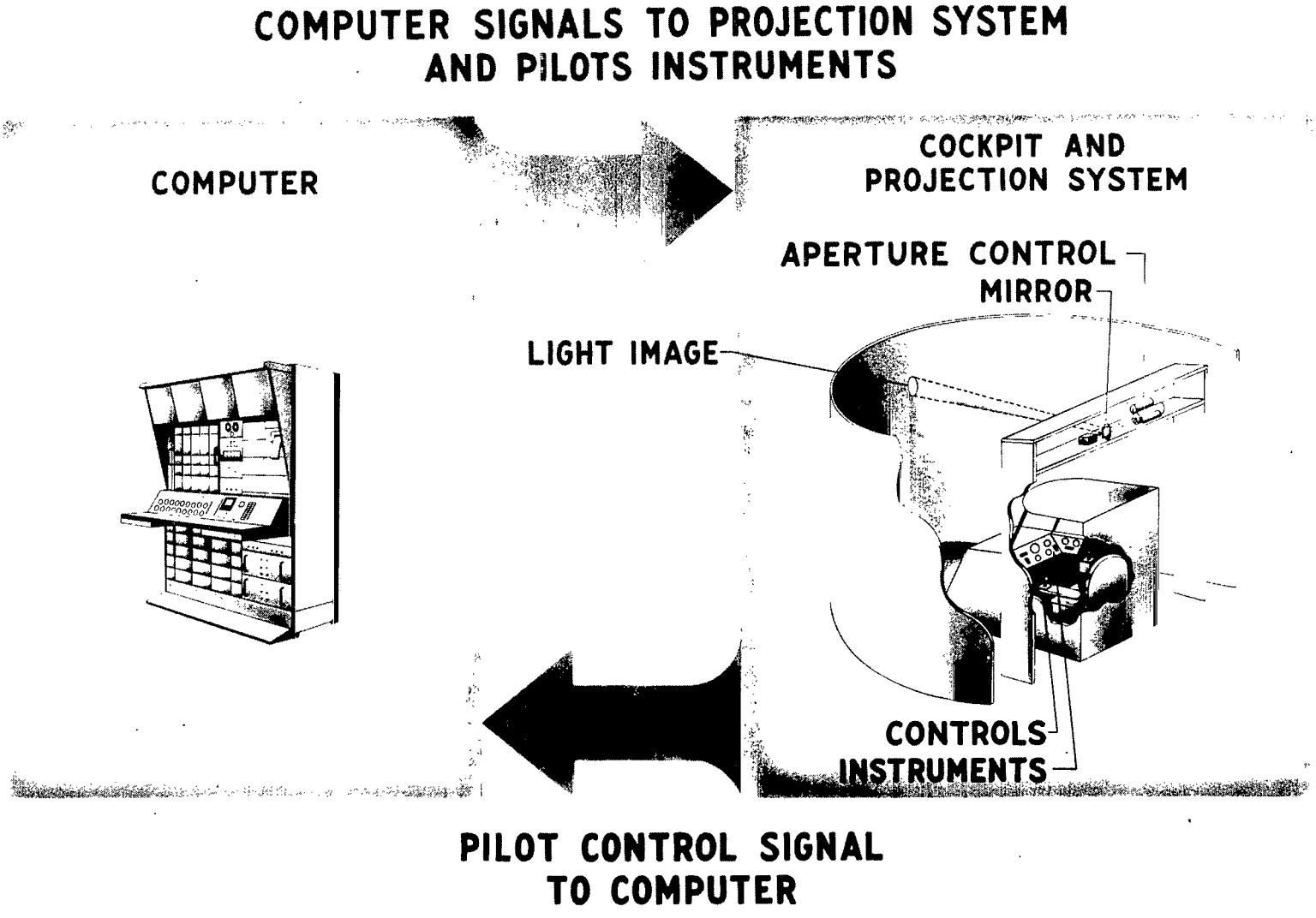

Figure 2.- Visual docking simulator.

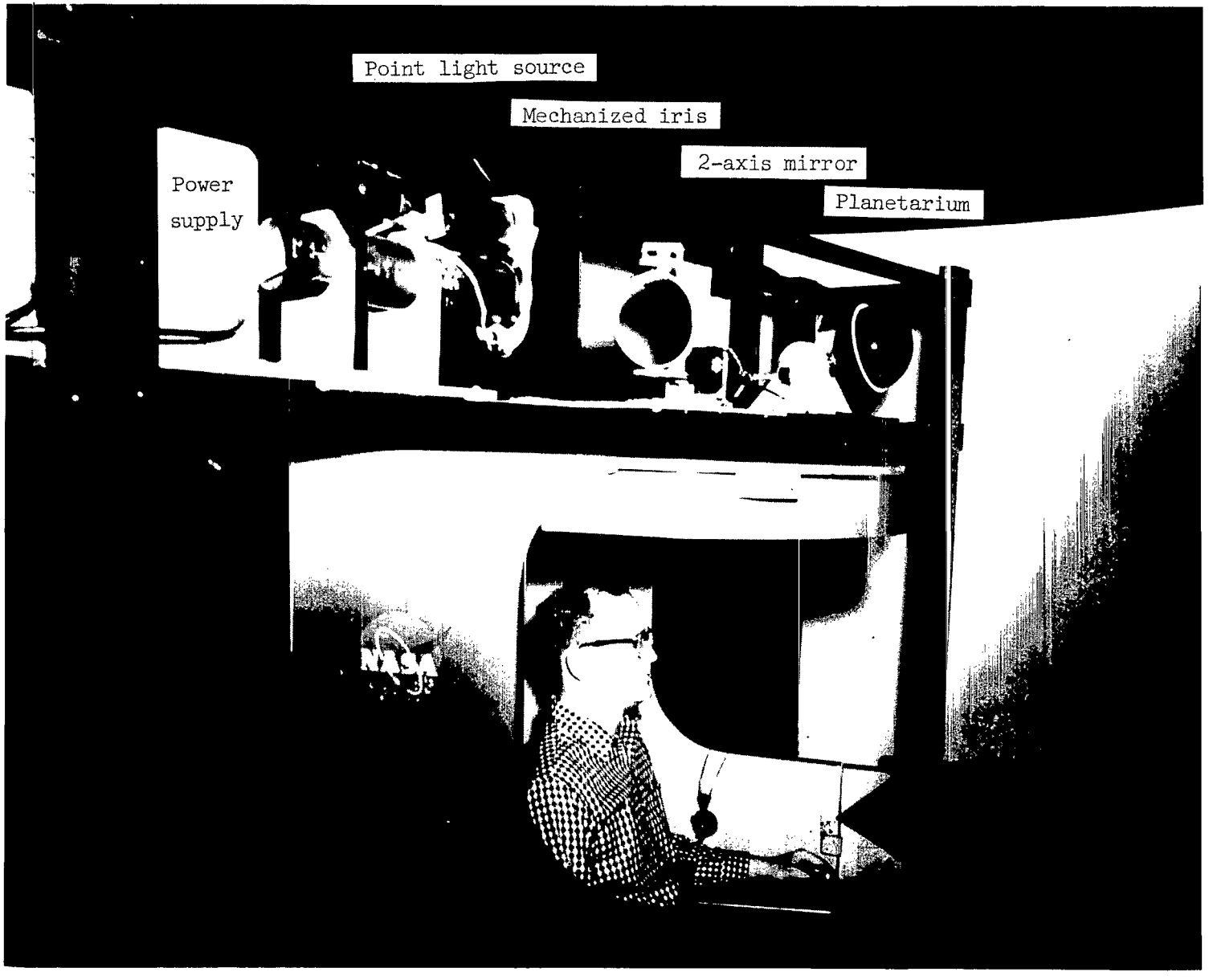

Figure 3.- Photograph of actual simulator showing projection system. L-63-4759

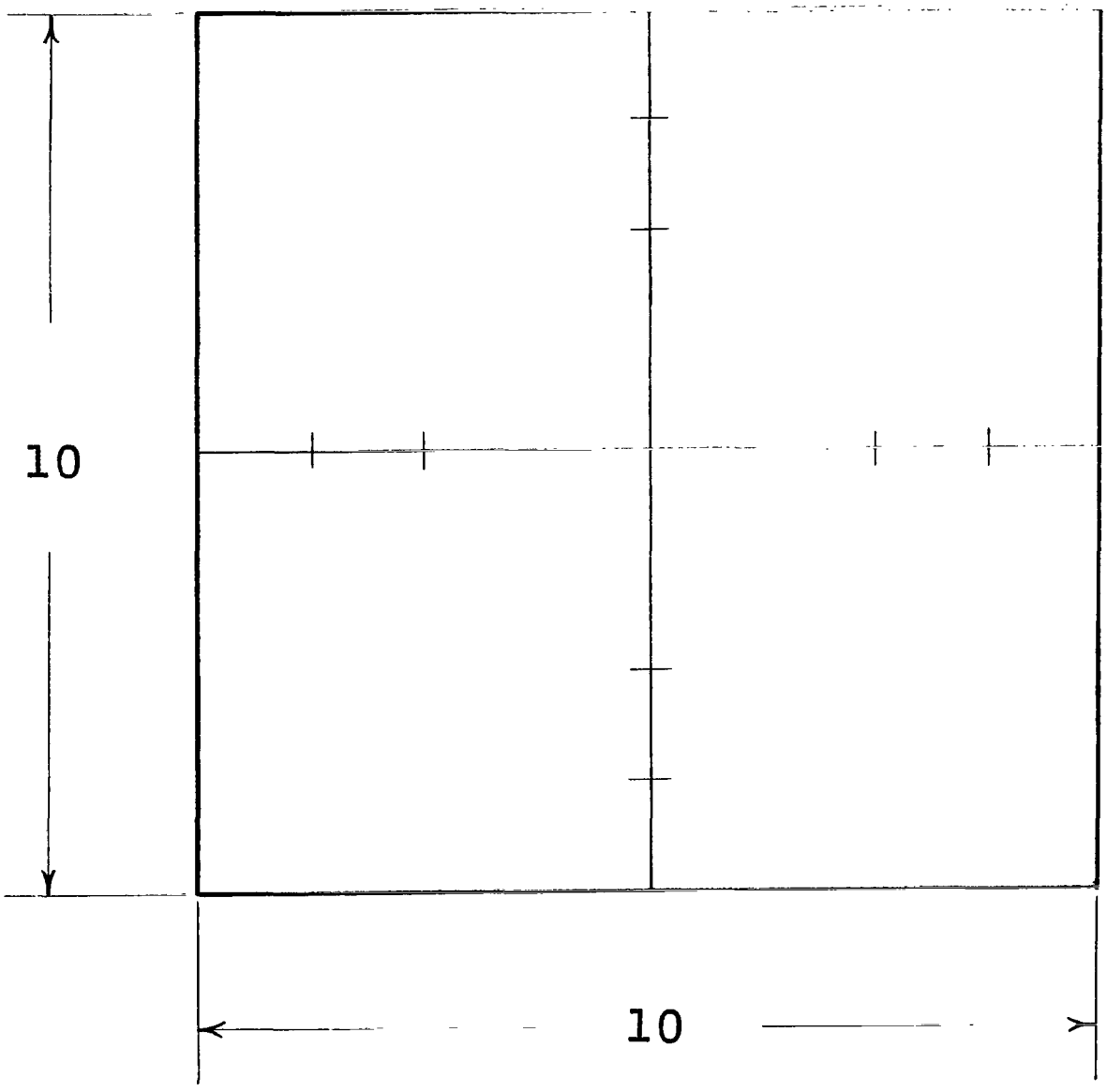

Figure 4.- Sketch of target. Dimensions are in inches.

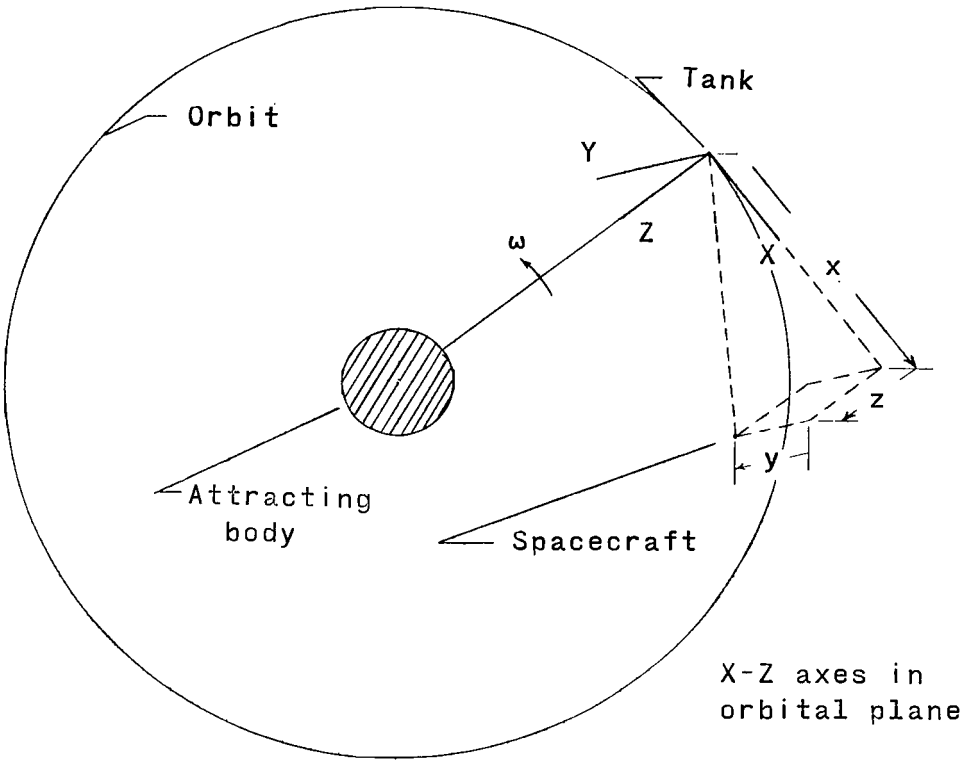

(a) Rotating axis system.

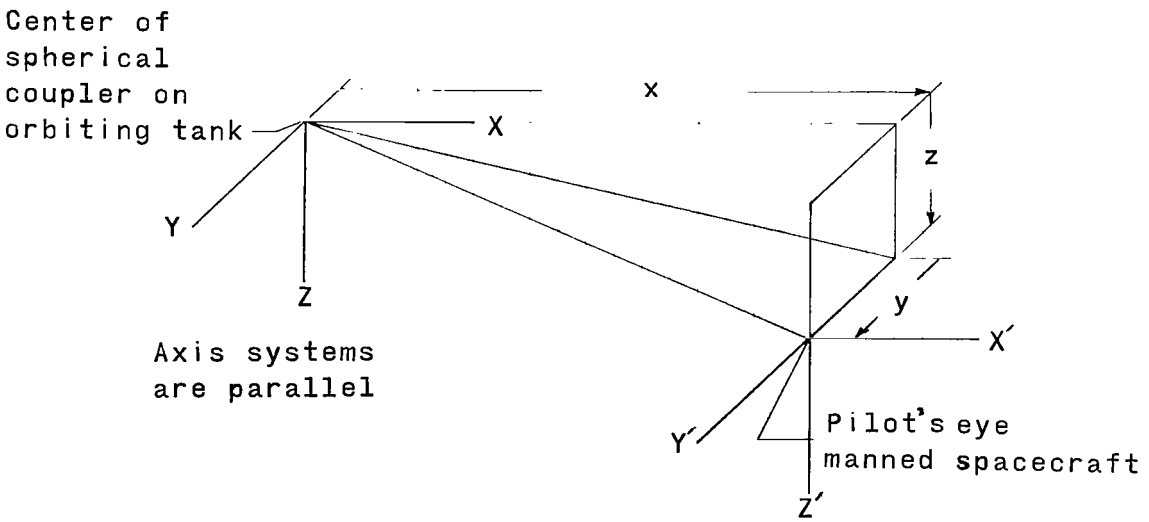

(b) Displacement and orientation of tank and spacecraft axes.

Figure 5.- Axes systems employed. Arrows indicate positive directions.

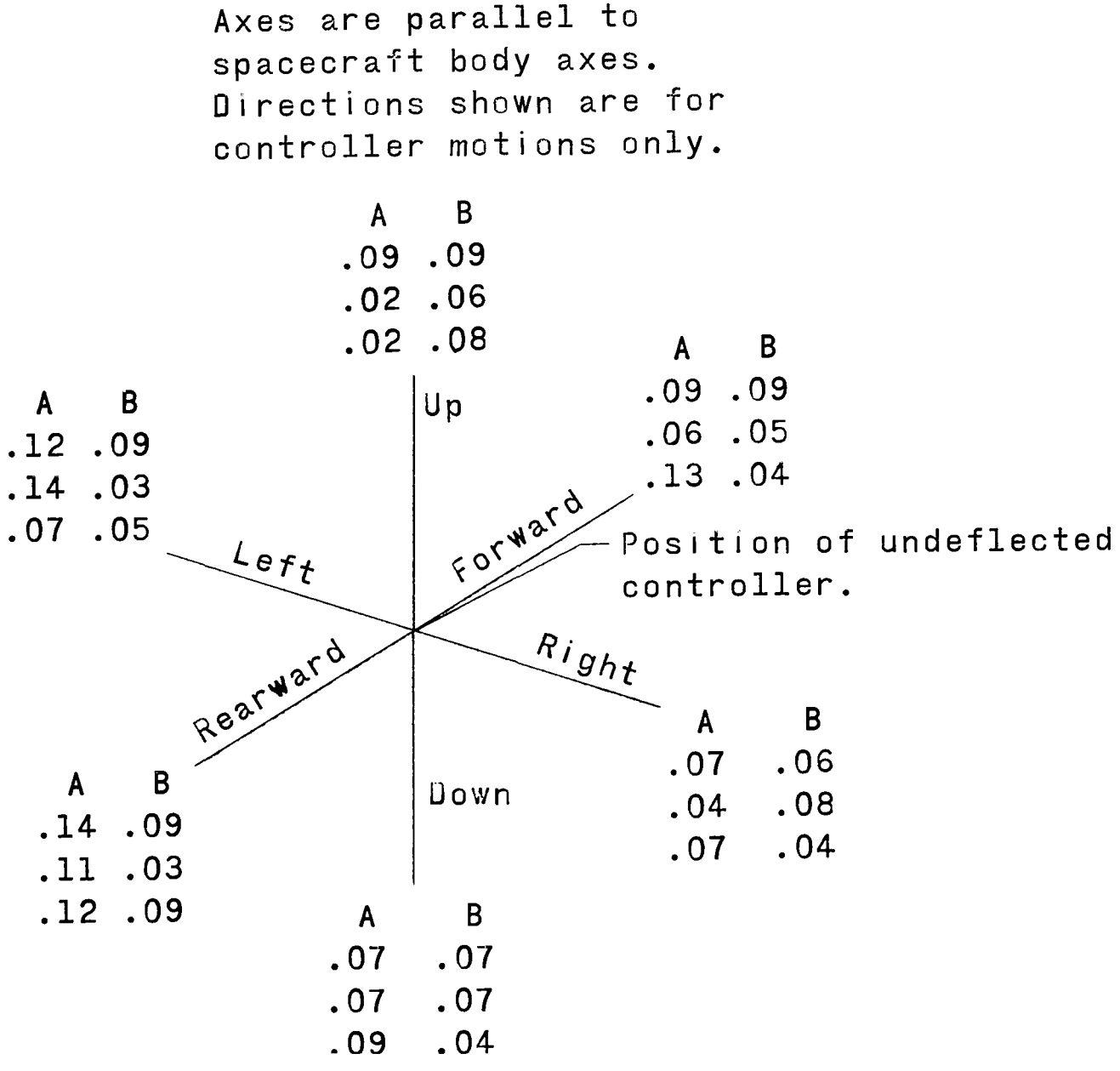

Figure 6.- Typical values of minimum time in seconds for controller inputs for two pilots (A and B) applying left-hand control with a three-axis finger-tip controller.

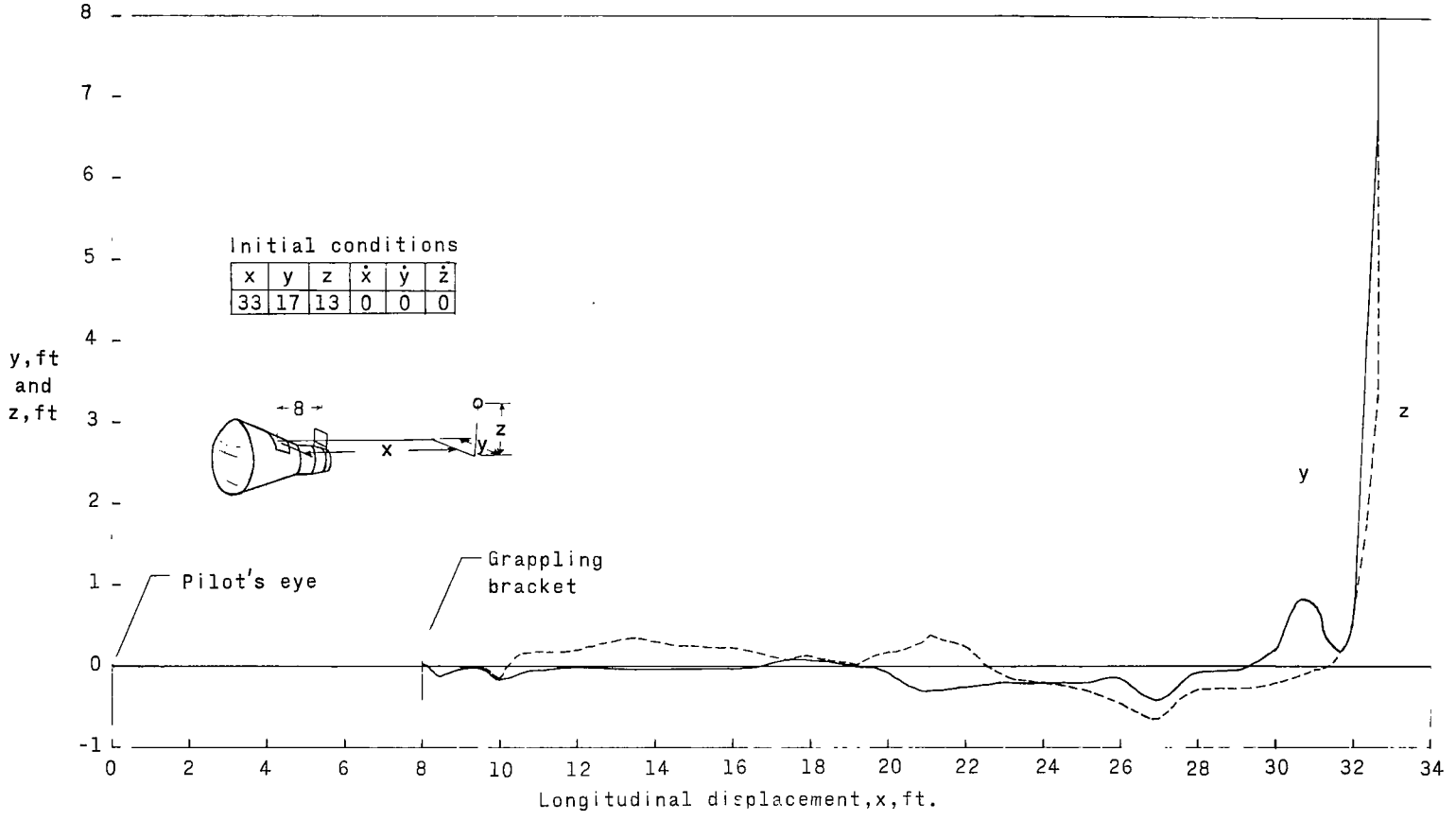

(a) Variation of vertical and lateral displacements of the center of the spherical ball coupler with distance along the line of sight through the center of the grappling bracket.

Figure 7.- Trajectory and time-history traces of a typical piloted flight that originated with initial range between spacecraft and tank approximately 40 feet and zero relative velocity. $T/m = 0.1$ ft/sec^2.

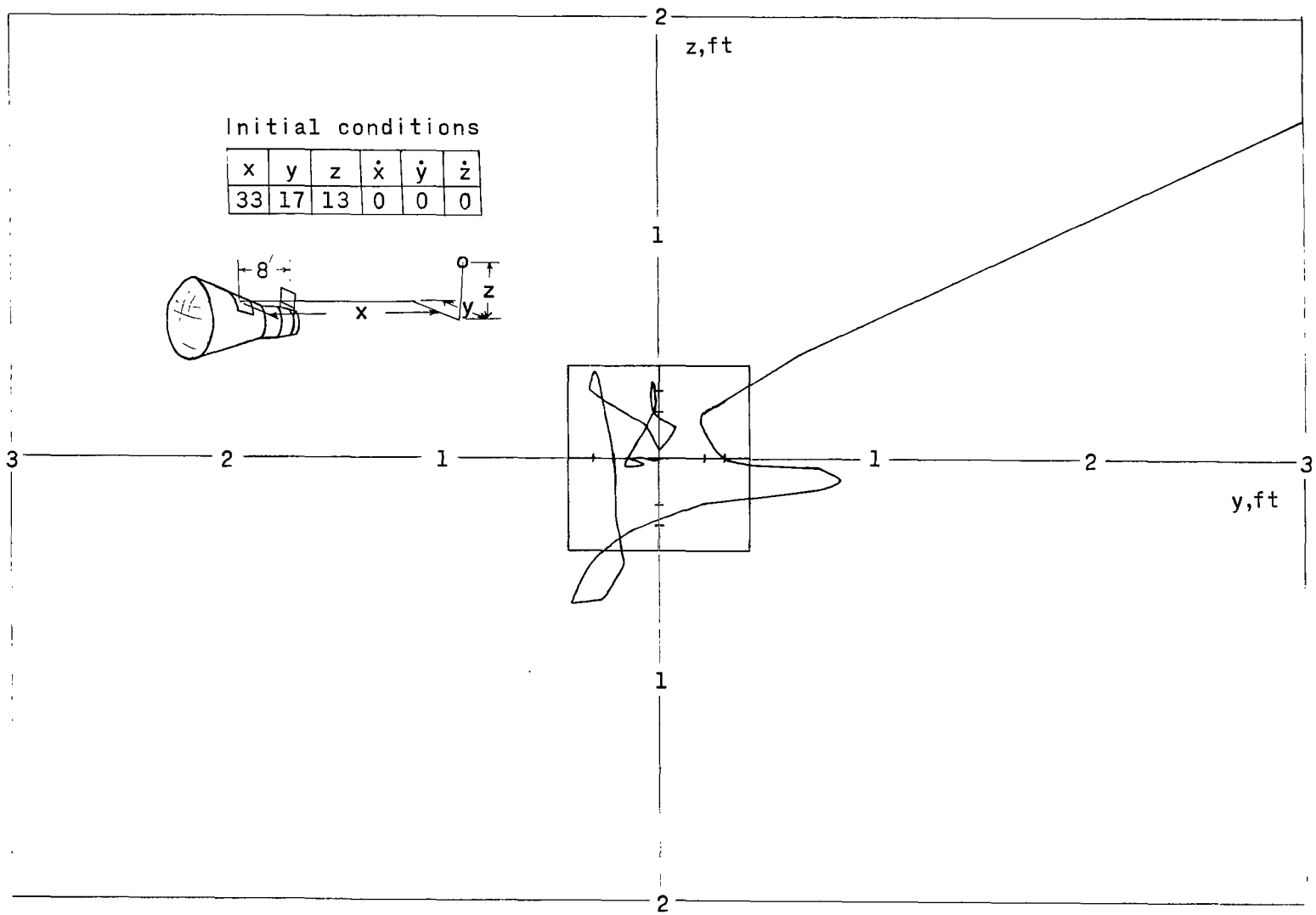

(b) Final portion of trajectory trace normal to line of sight through target center.

Figure 7.- Continued.

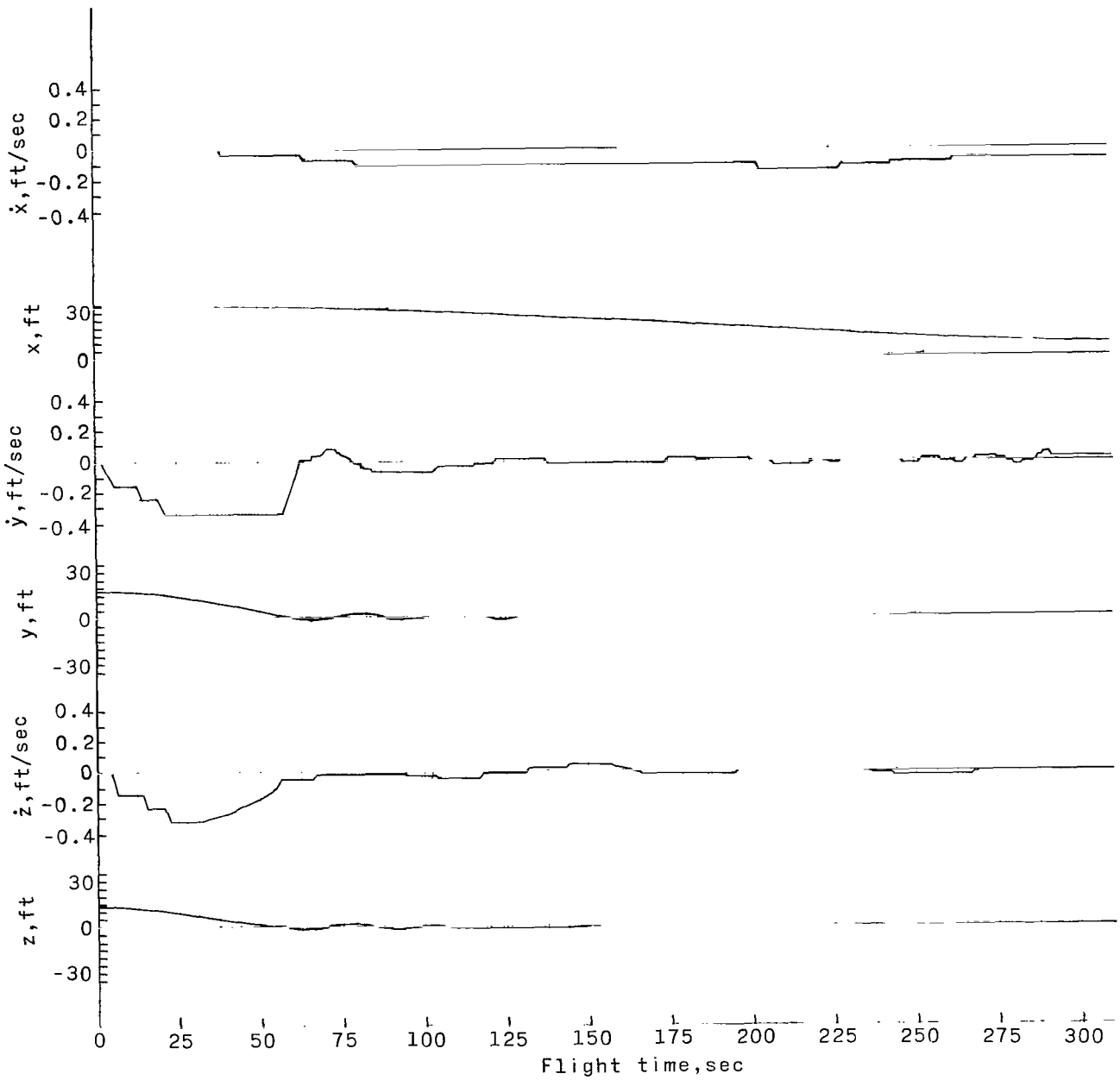

(c) Time-history traces.

Figure 7.- Concluded.

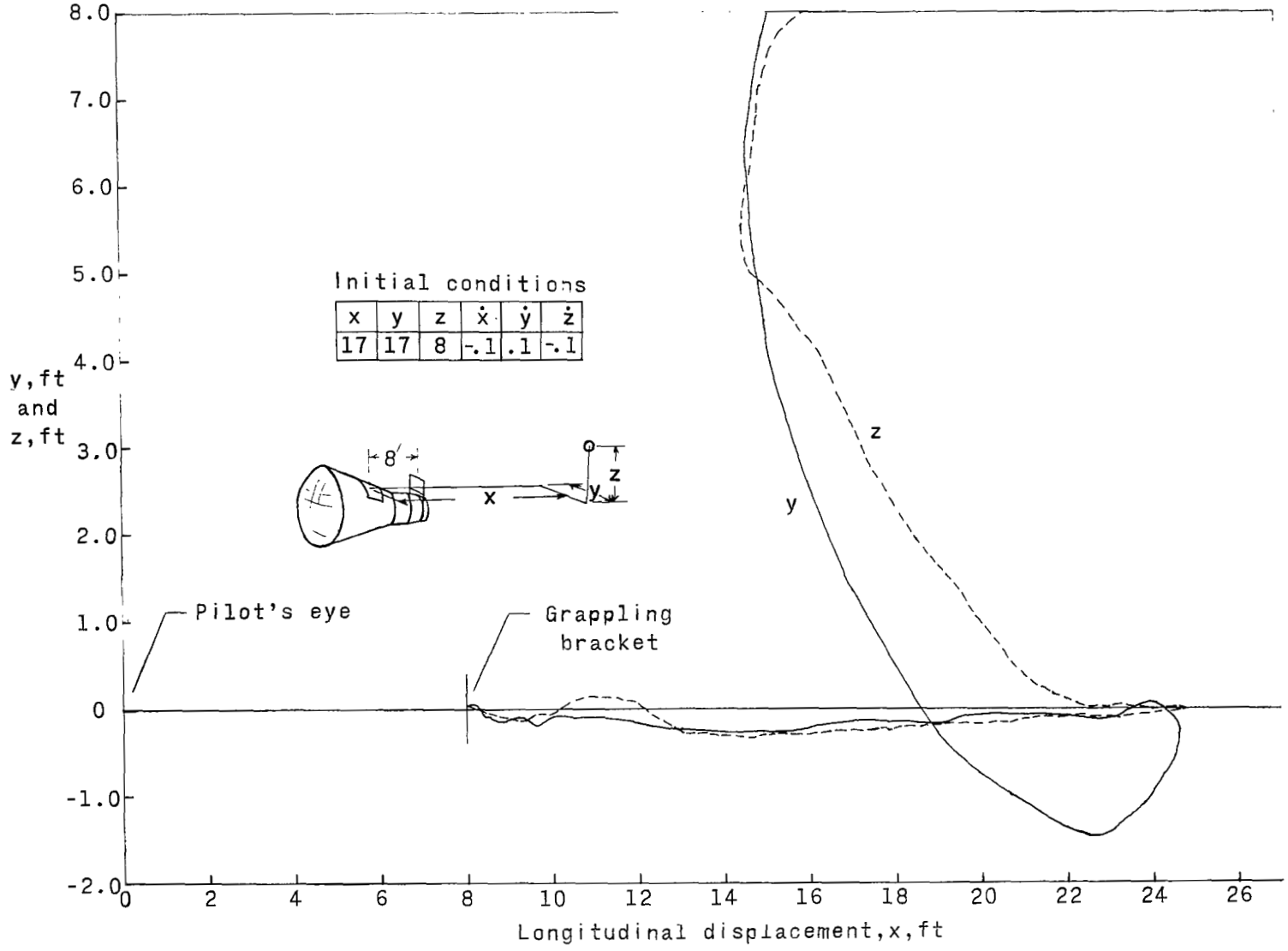

(a) Variation of vertical and lateral displacements of the center of the spherical ball coupler with distance along the line of sight through the center of the grappling bracket.

Figure 8.- Trajectory and time-history traces for a piloted flight that originated at a range of 25 feet with small initial velocities along each axis. $T/m = 0.2$ ft/sec^2.

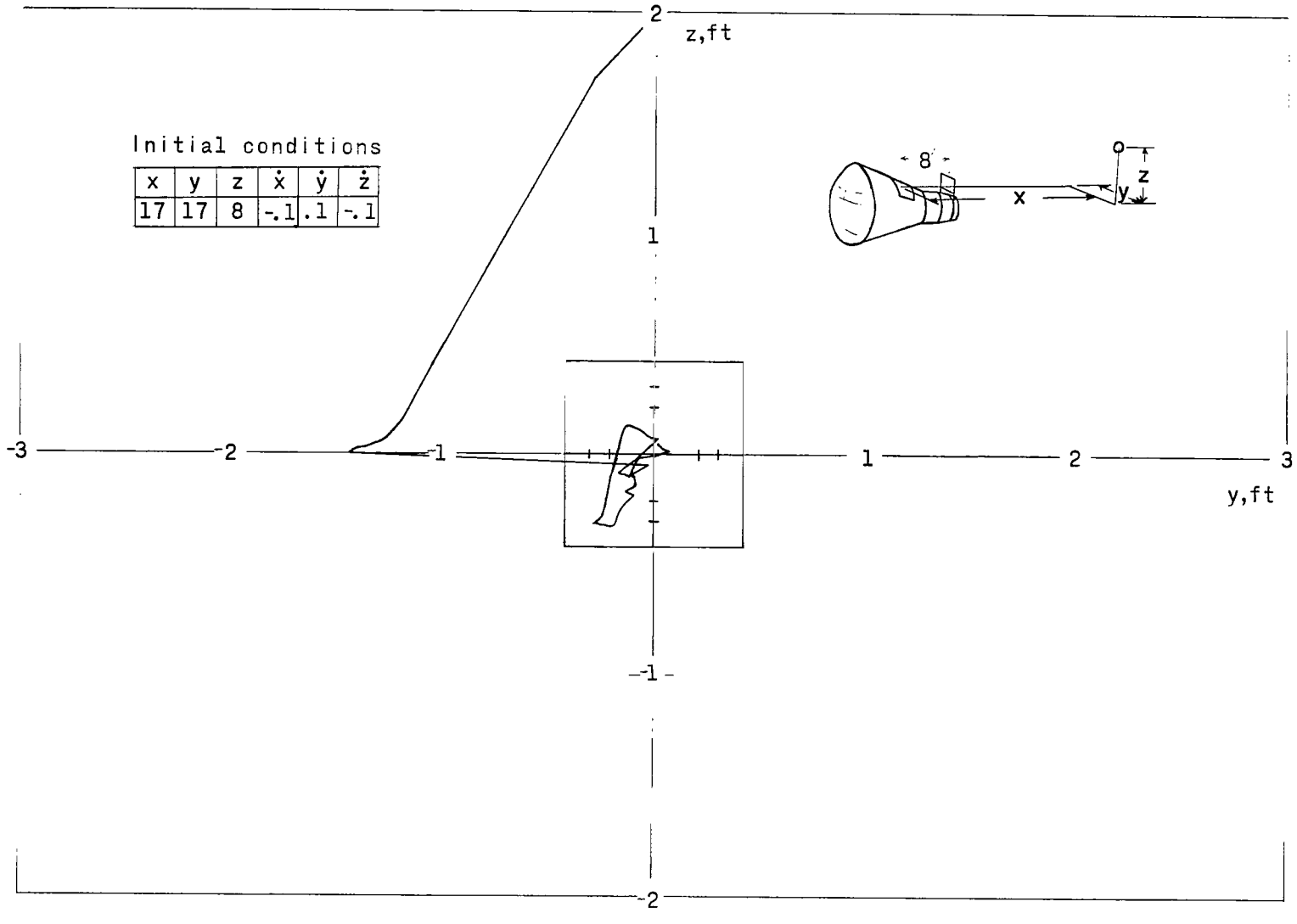

(b) Final portion of trajectory trace normal to line of sight through target center.

Figure 8.- Continued.

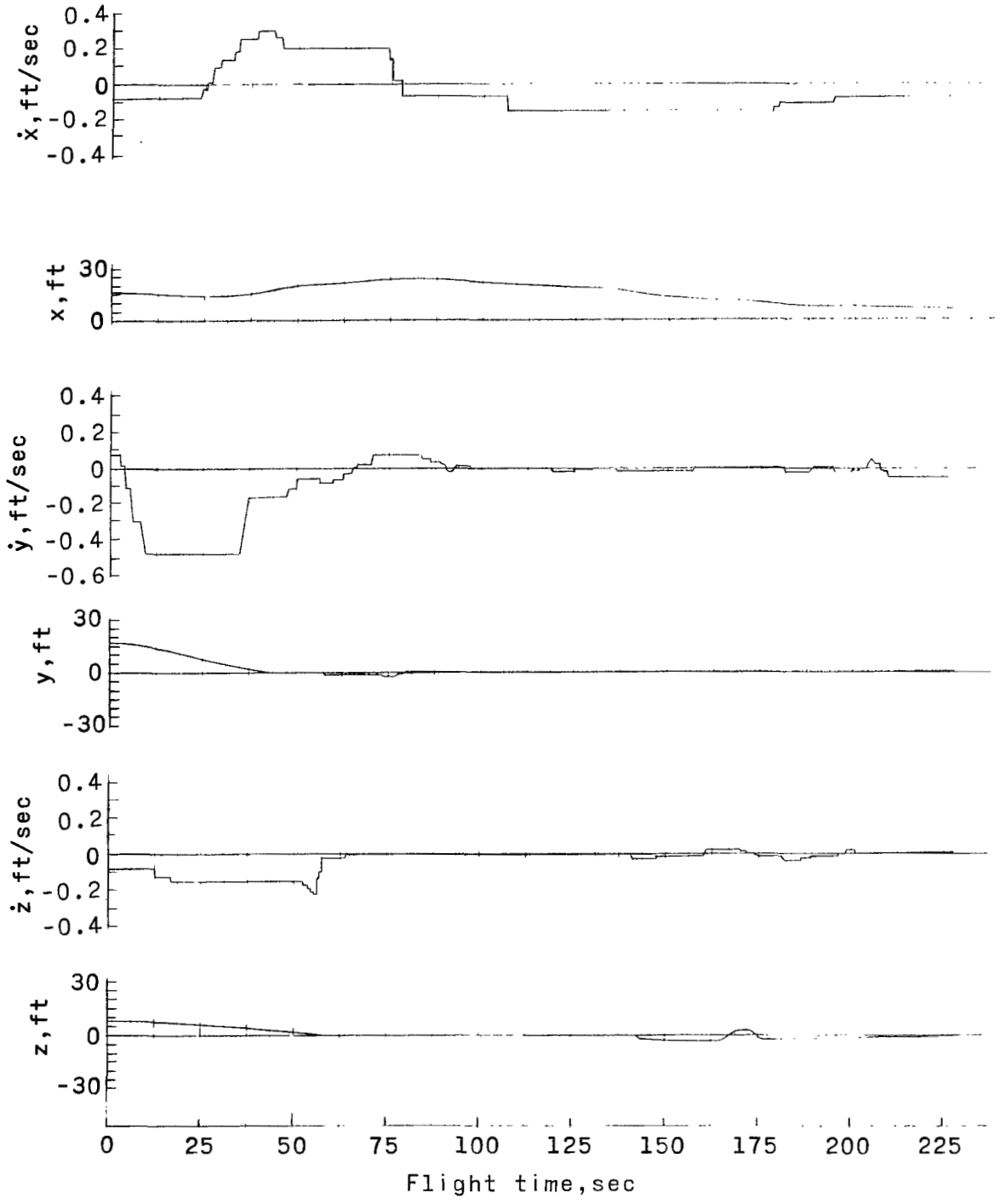

(c) Time-history traces.

Figure 8.- Concluded.

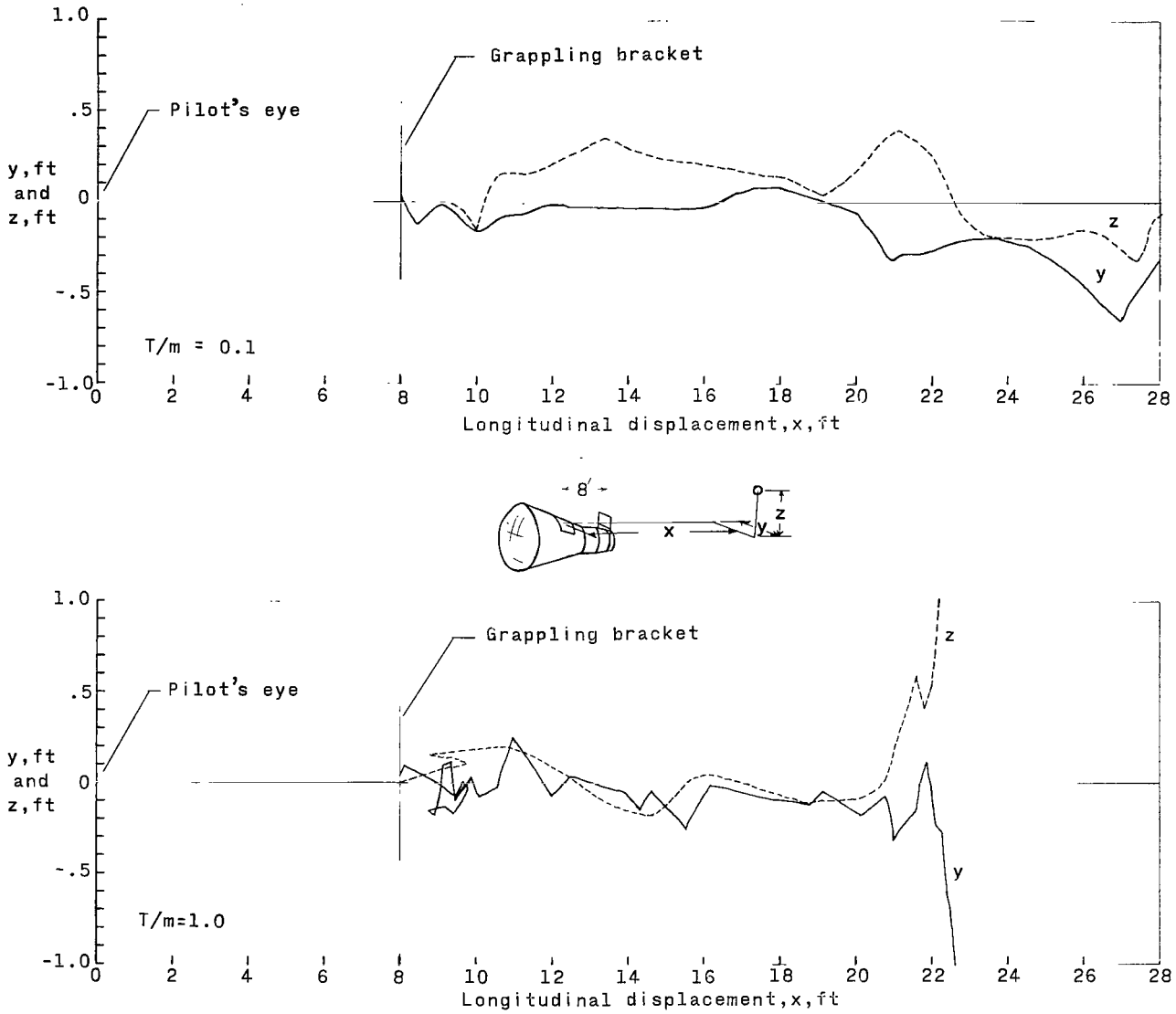

Figure 9.- Final portion of the trajectory traces for two piloted flights illustrating the effect of control acceleration level.

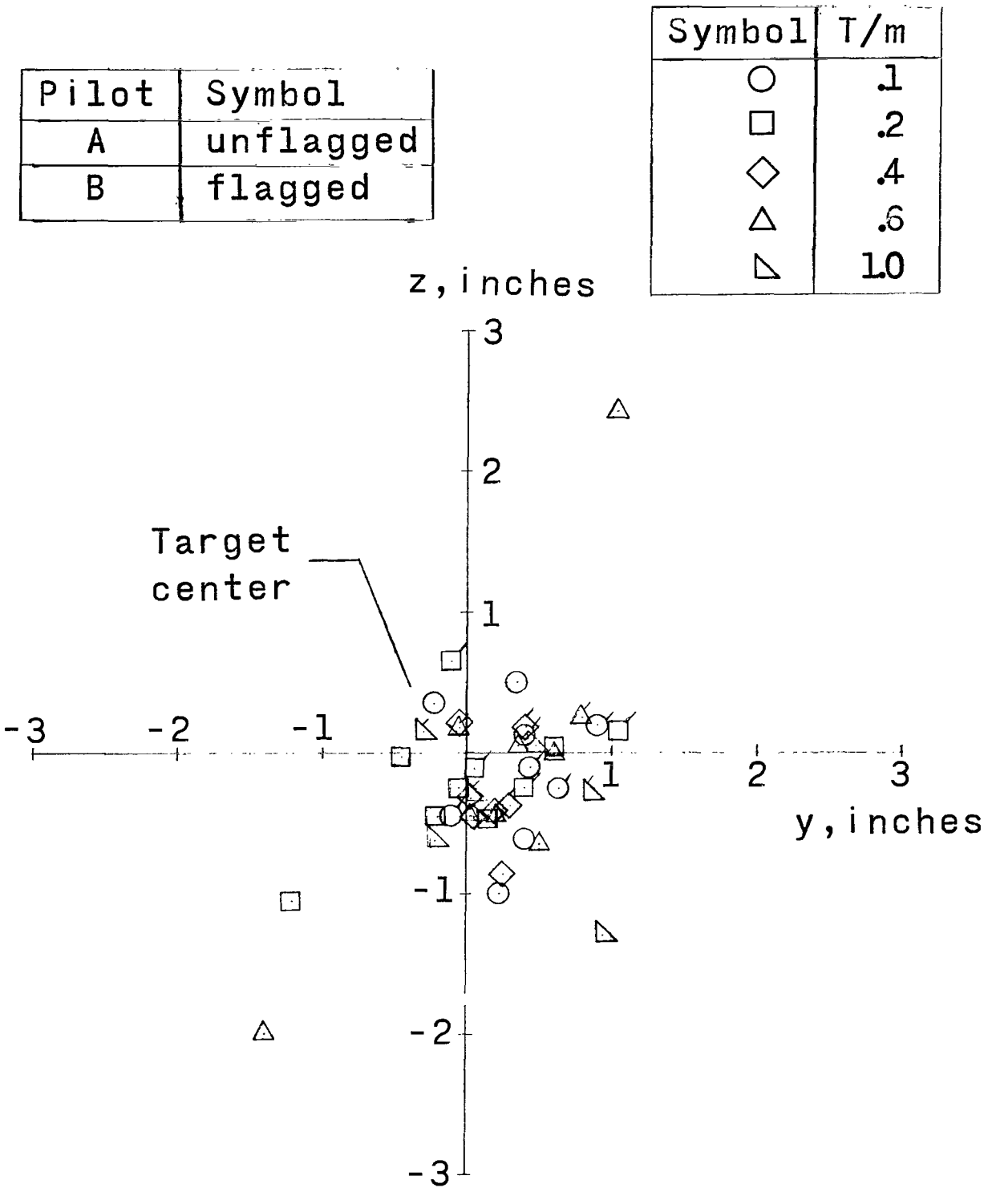

Figure 10.- Displacement of center of light spot from the center of the target at contact of the coupling mechanism.

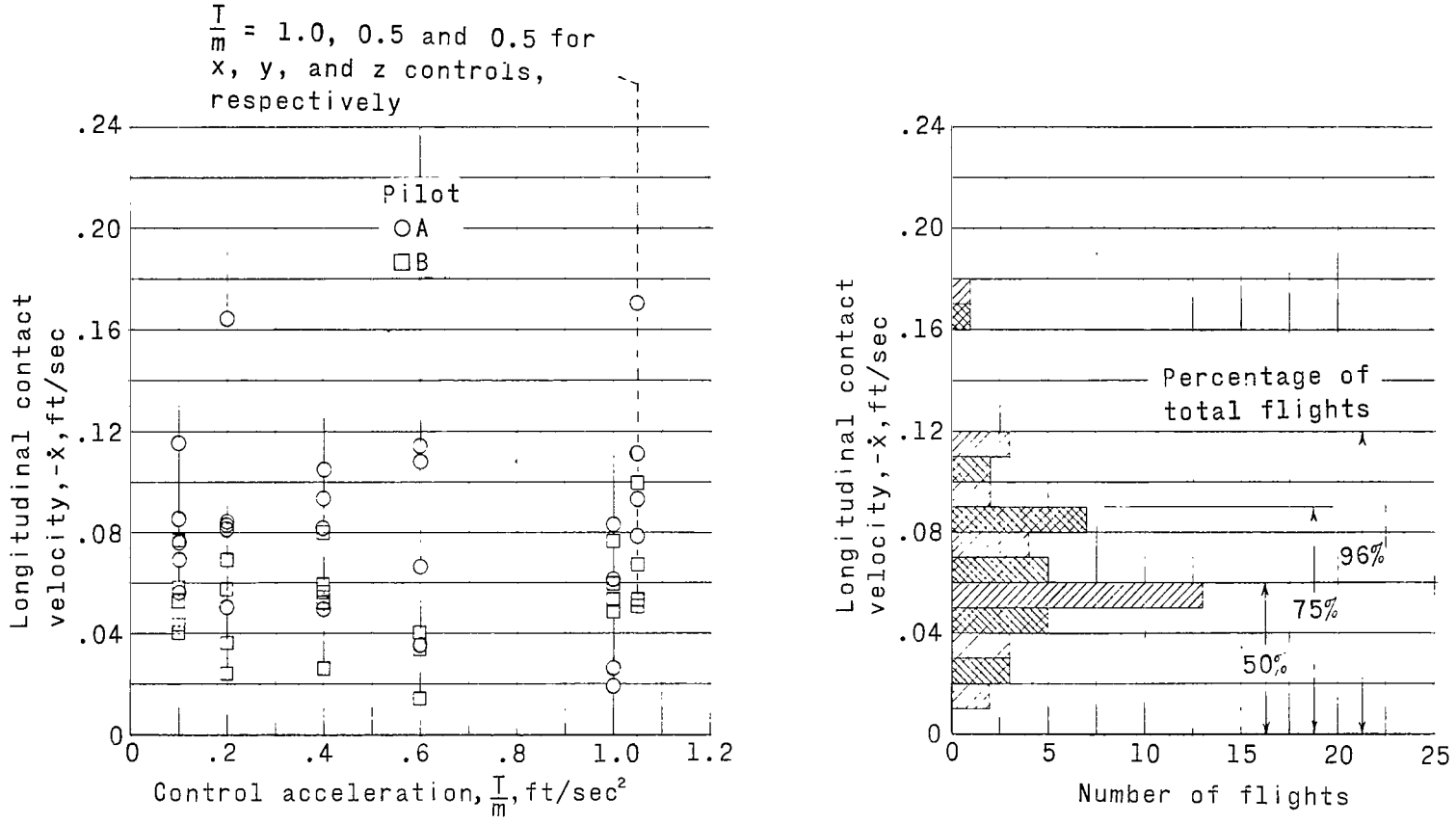

(a) Longitudinal contact velocity.

Figure 11.- Contact velocity between couplers as a function of acceleration level of the controls.

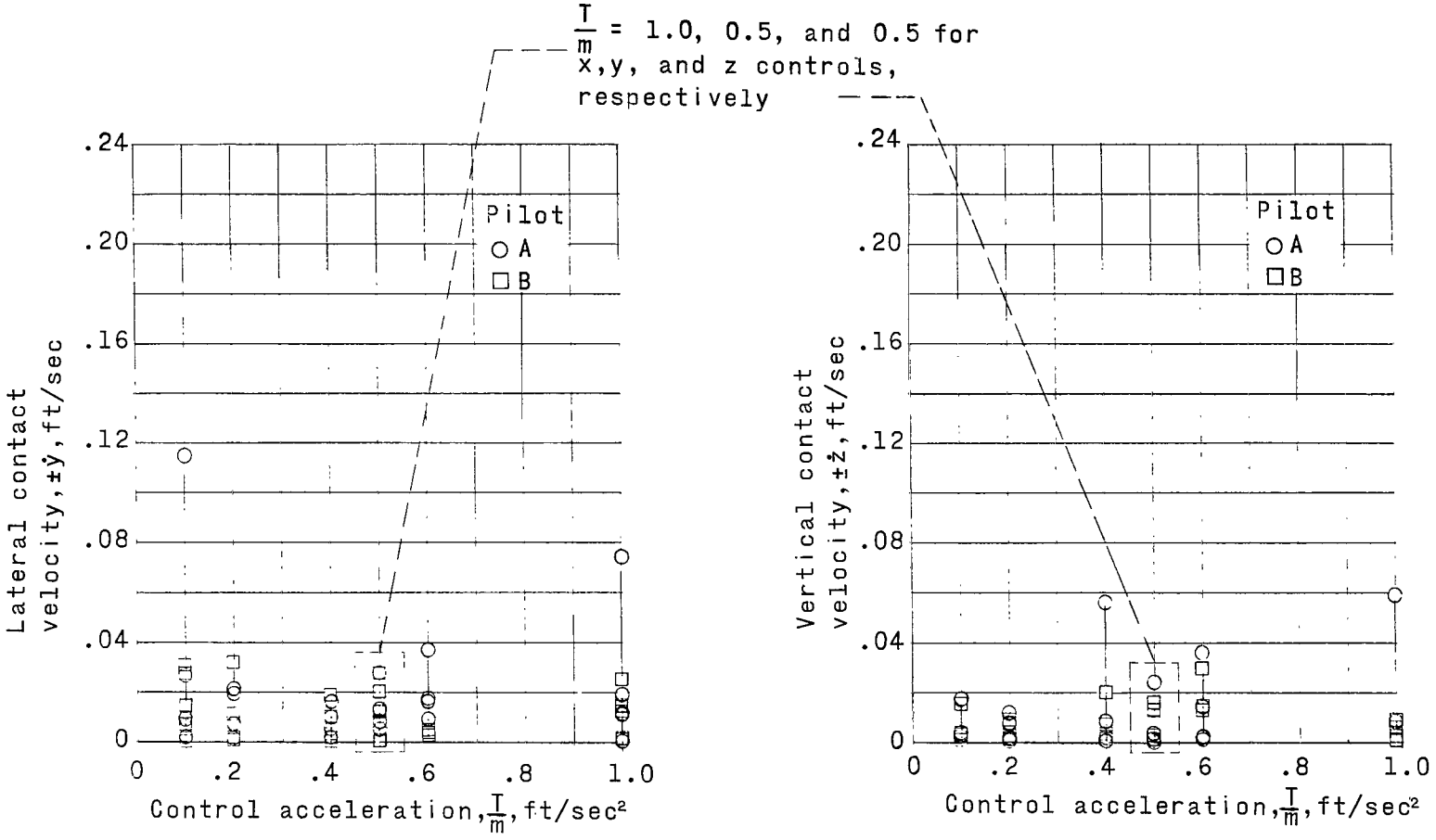

(b) Lateral and vertical contact velocities.

Figure 11.- Concluded.

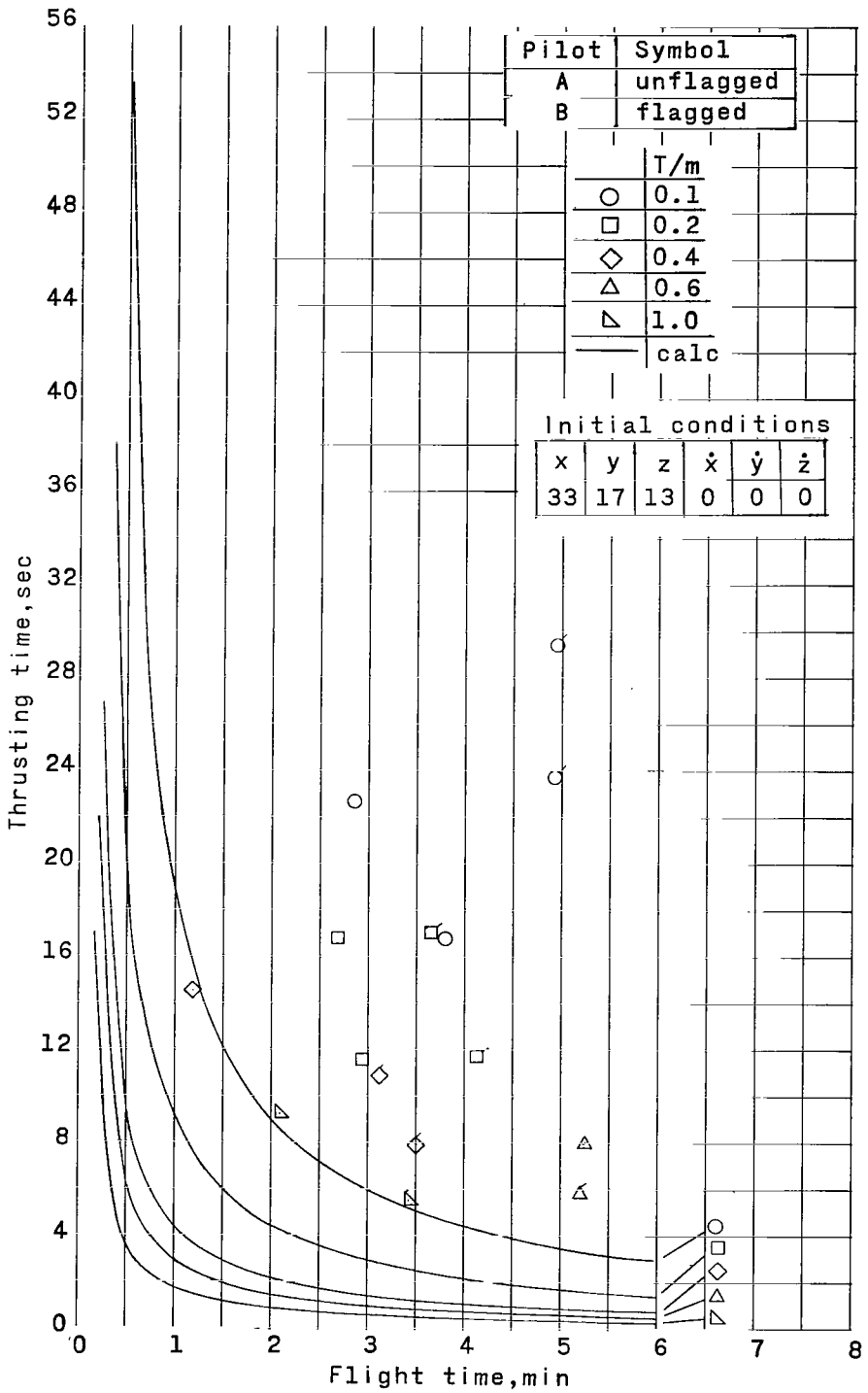

Figure 12.- Variation of total thrusting time with flight time for different values of control acceleration.

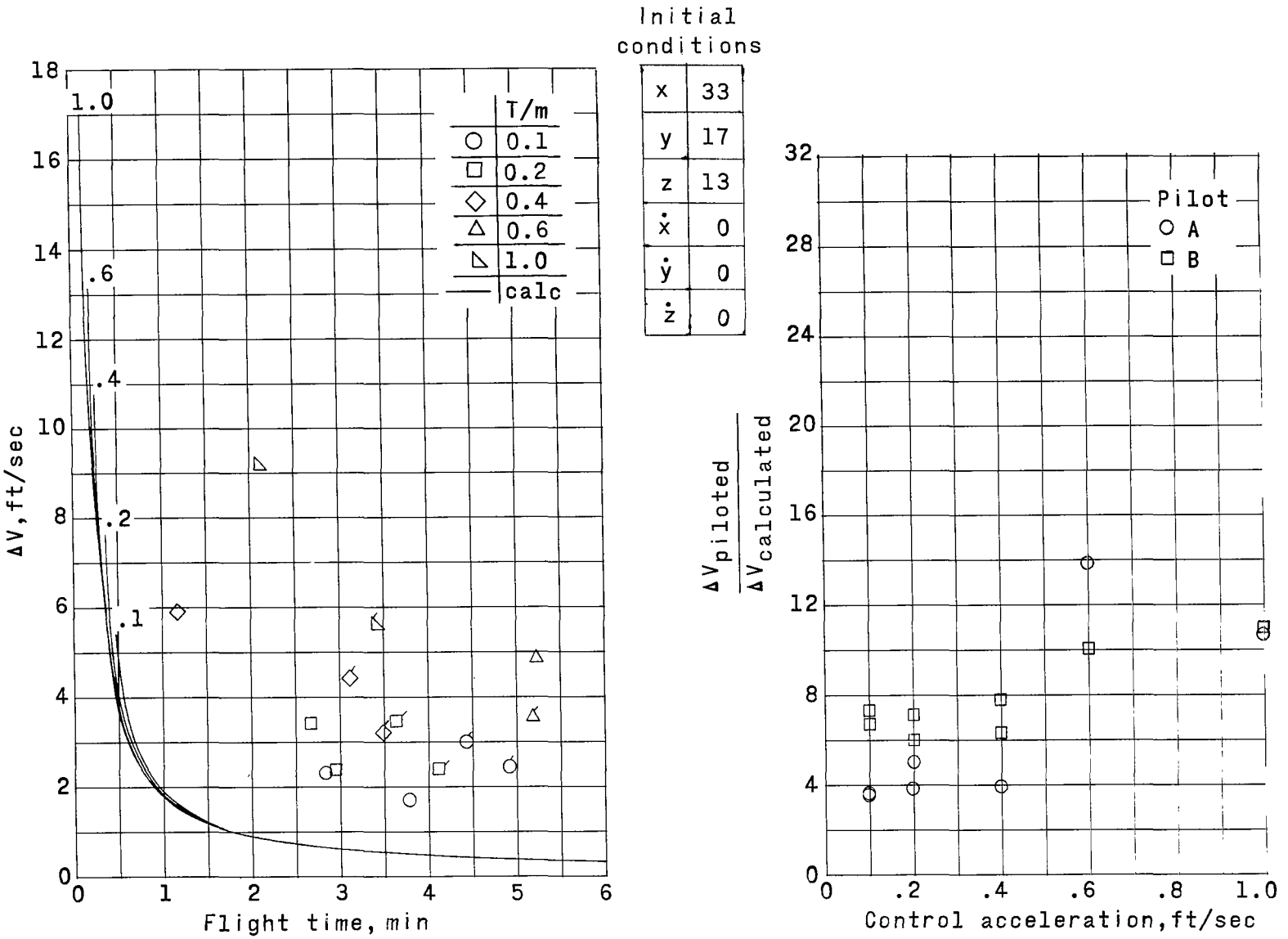

Figure 13.- Characteristic velocity ΔV as a function of flight time for various values of control acceleration and the ratio of piloted to calculated ΔV as a function of control acceleration.

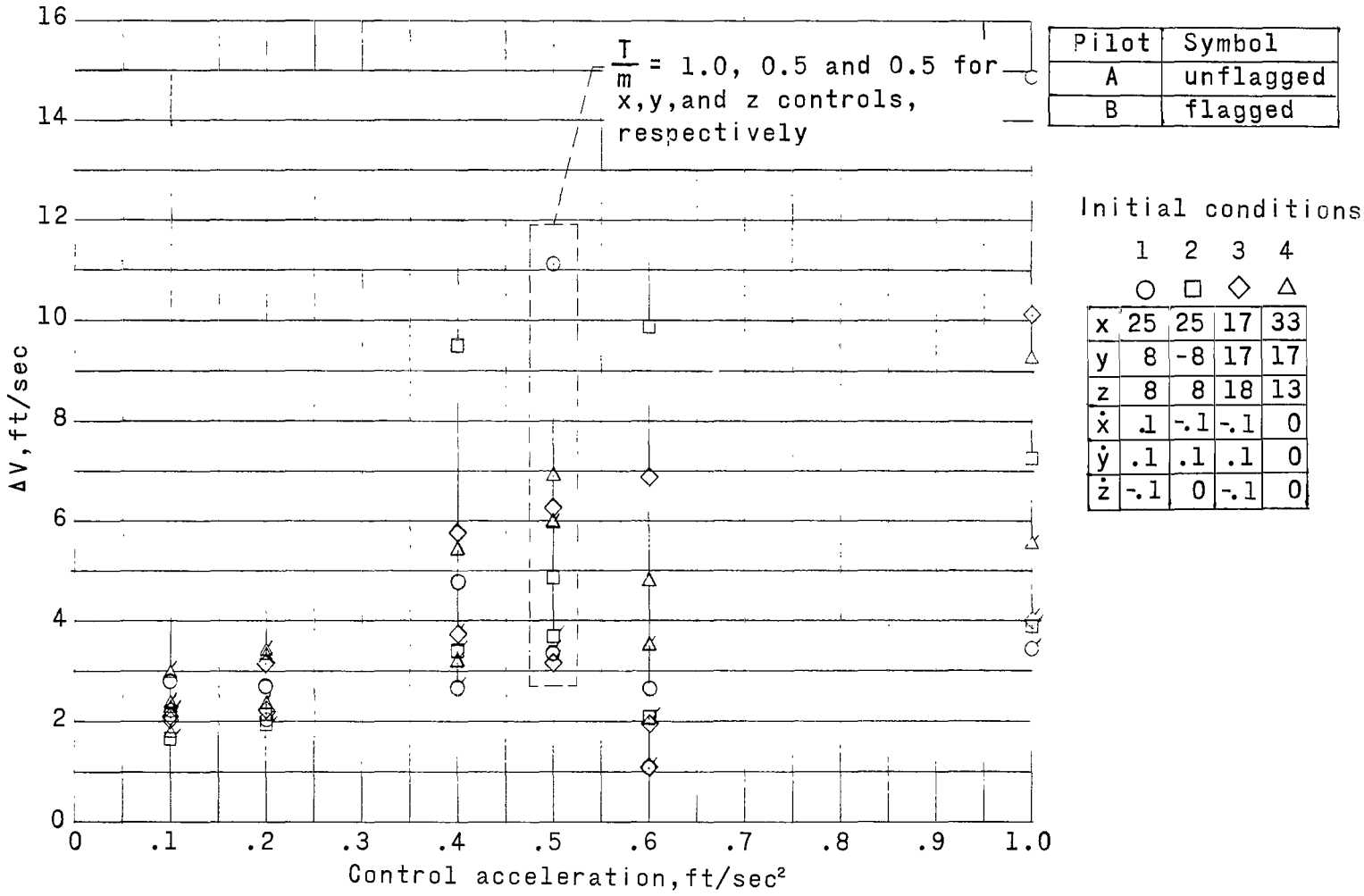

Figure 14.- Characteristic velocity ΔV used in docking plotted against control acceleration level for four sets of initial conditions.

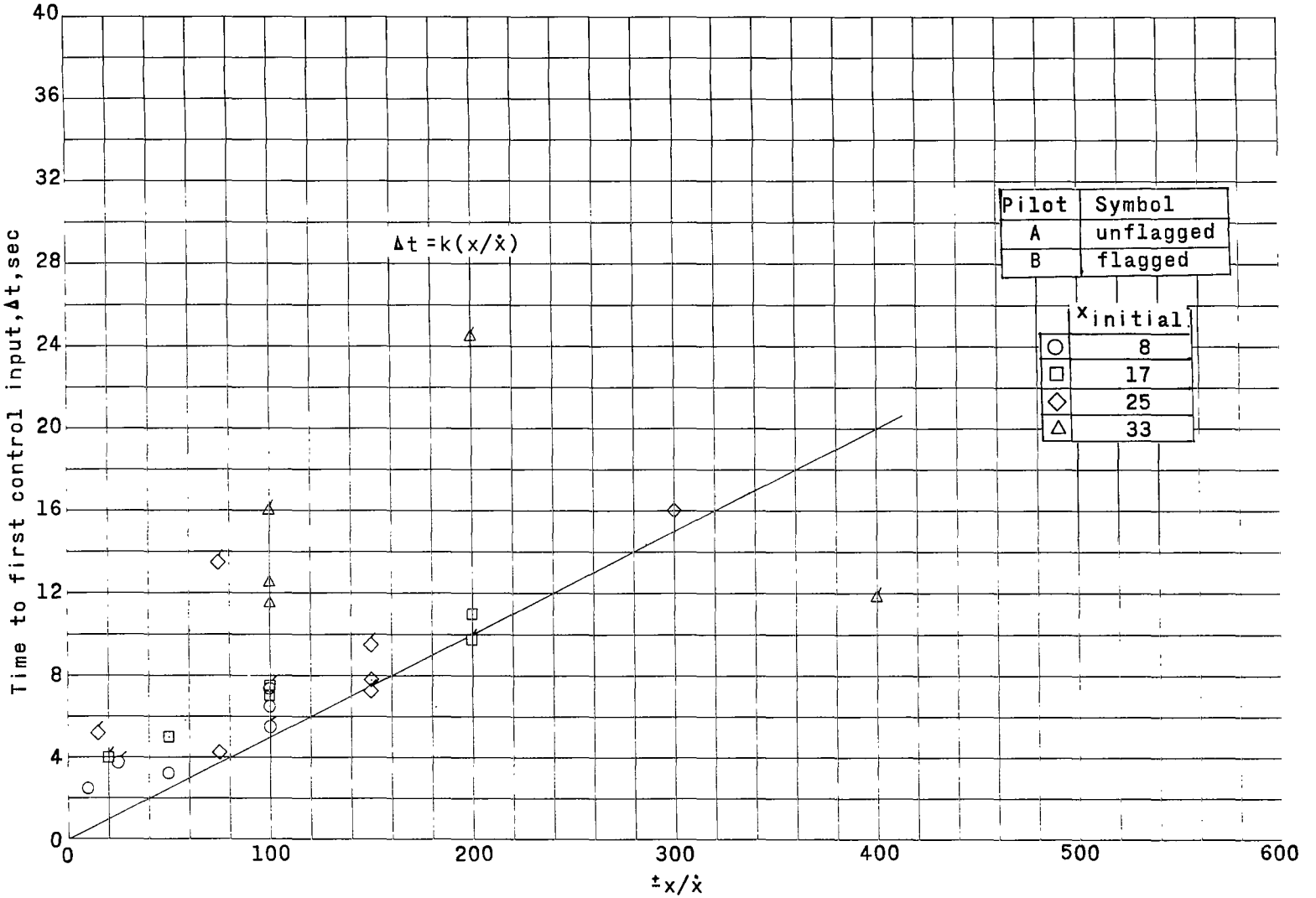

Figure 15.- Observation time to first control input plotted against initial values of the ratio $x/\dot{x}$ for single-axis supplemental tests.

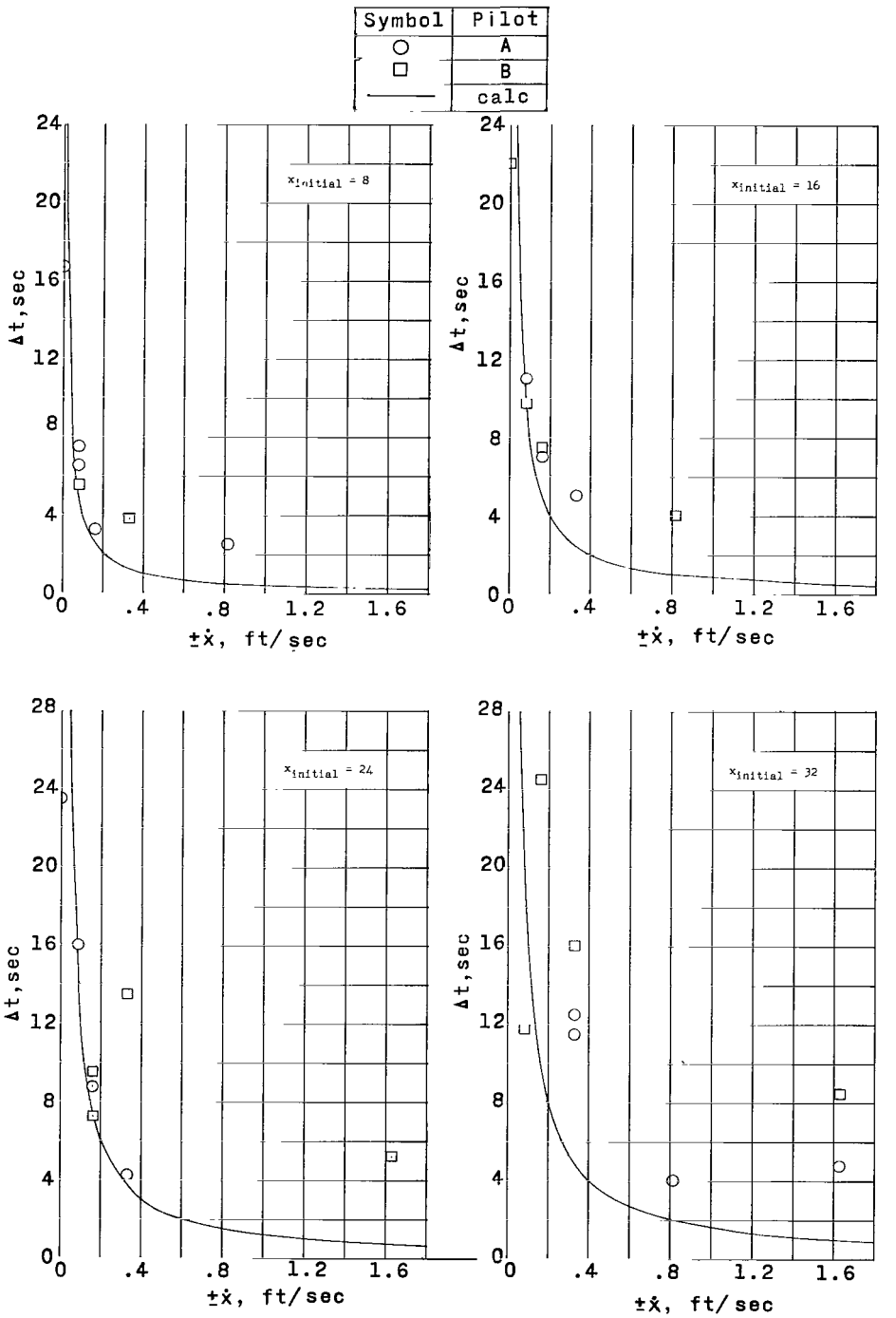

Figure 16.- Comparison of experimental and calculated values of observation time (Δt from problem initiation to first control input) plotted against initial closing velocity for single-axis supplemental tests. $T/m = 0.1$ ft/sec^2 and $k = 0.05$.

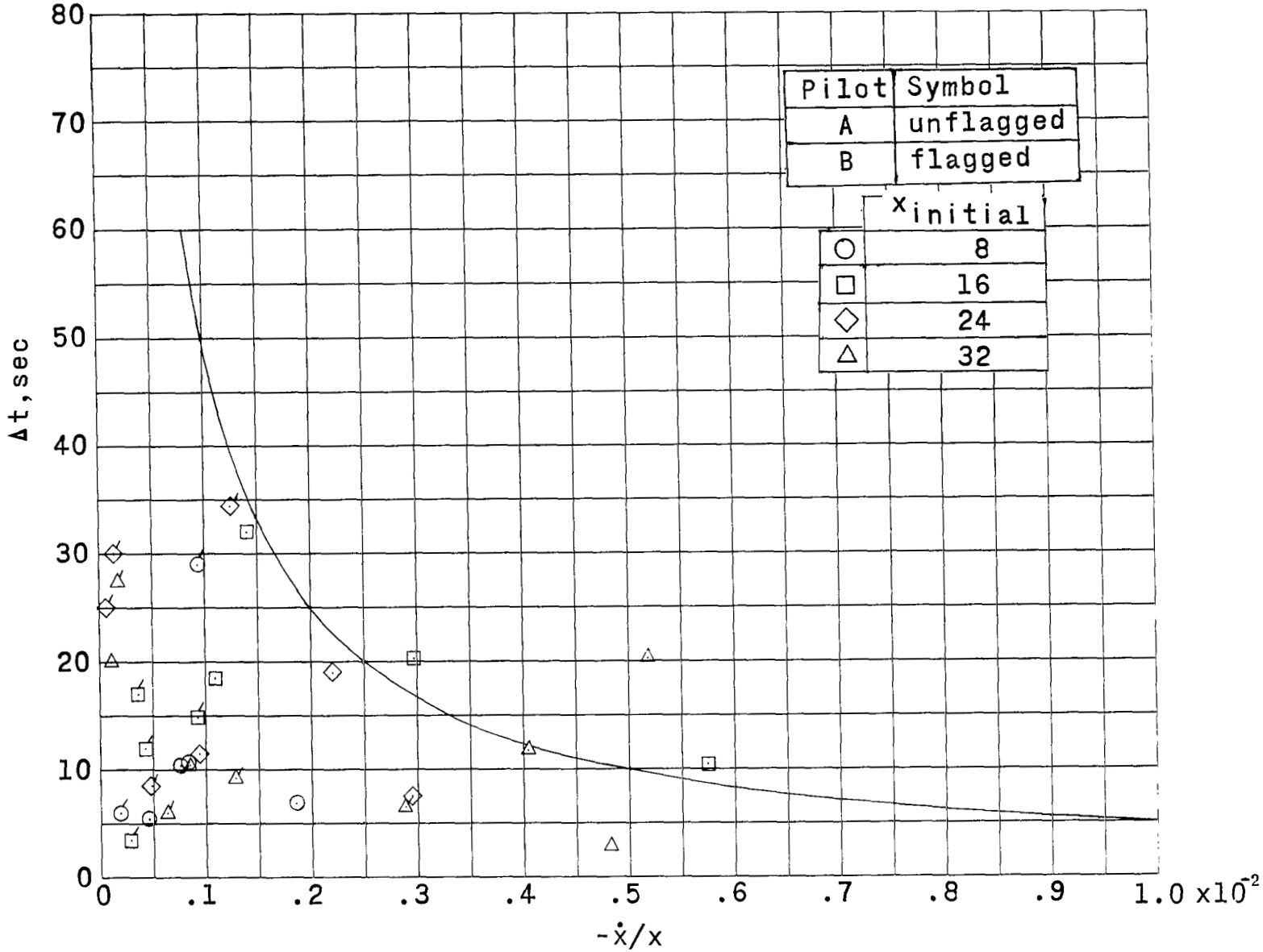

Figure 17.- Comparison of experimental and calculated values of observation time Δt from last control input to end of flight plotted against the ratio $\dot{x}/x$ for single-axis supplemental tests. $T/m = 0.1$ ft/sec^2.

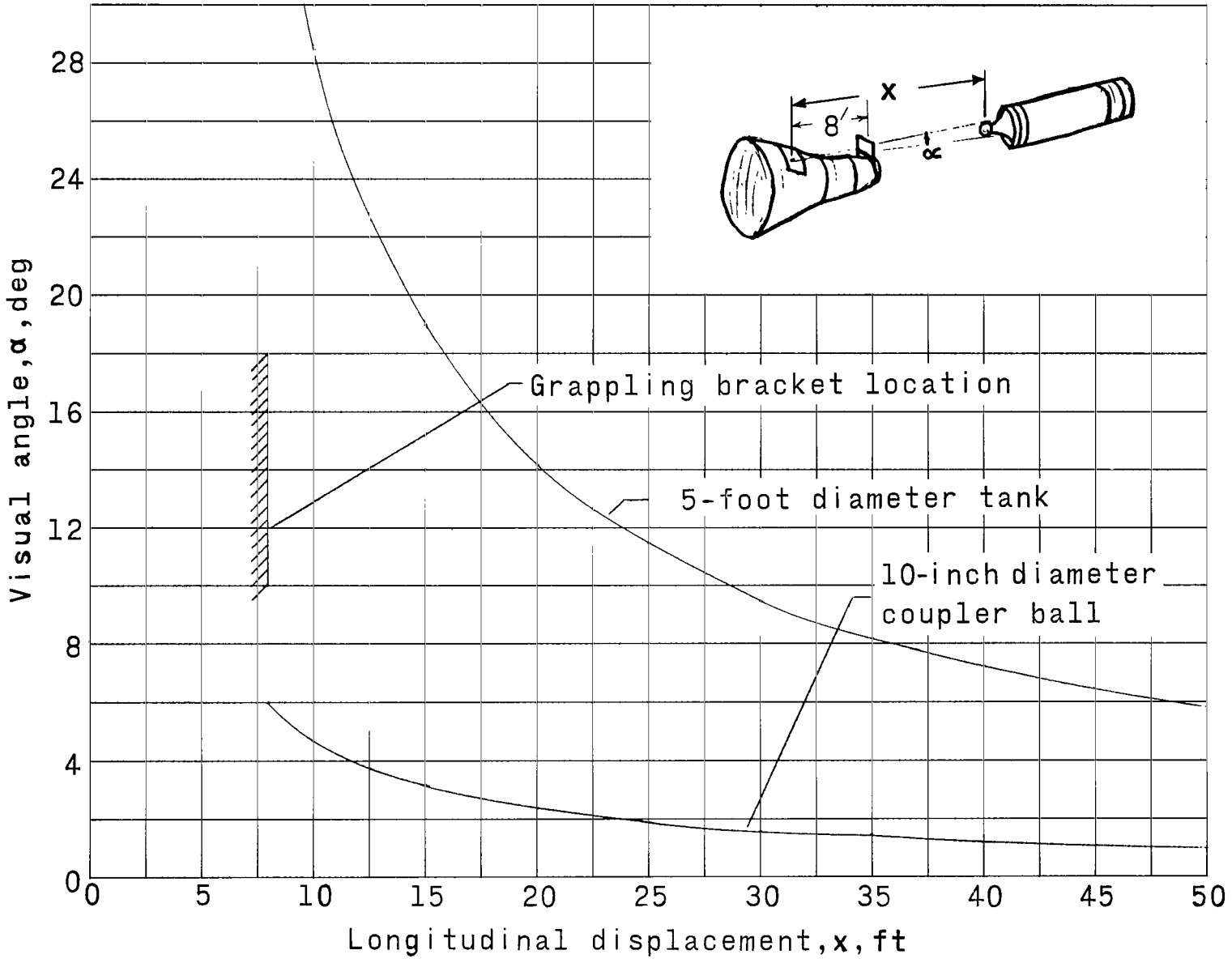

Figure 18.- Variation of visual angle with longitudinal separation distance for configuration illustrated.

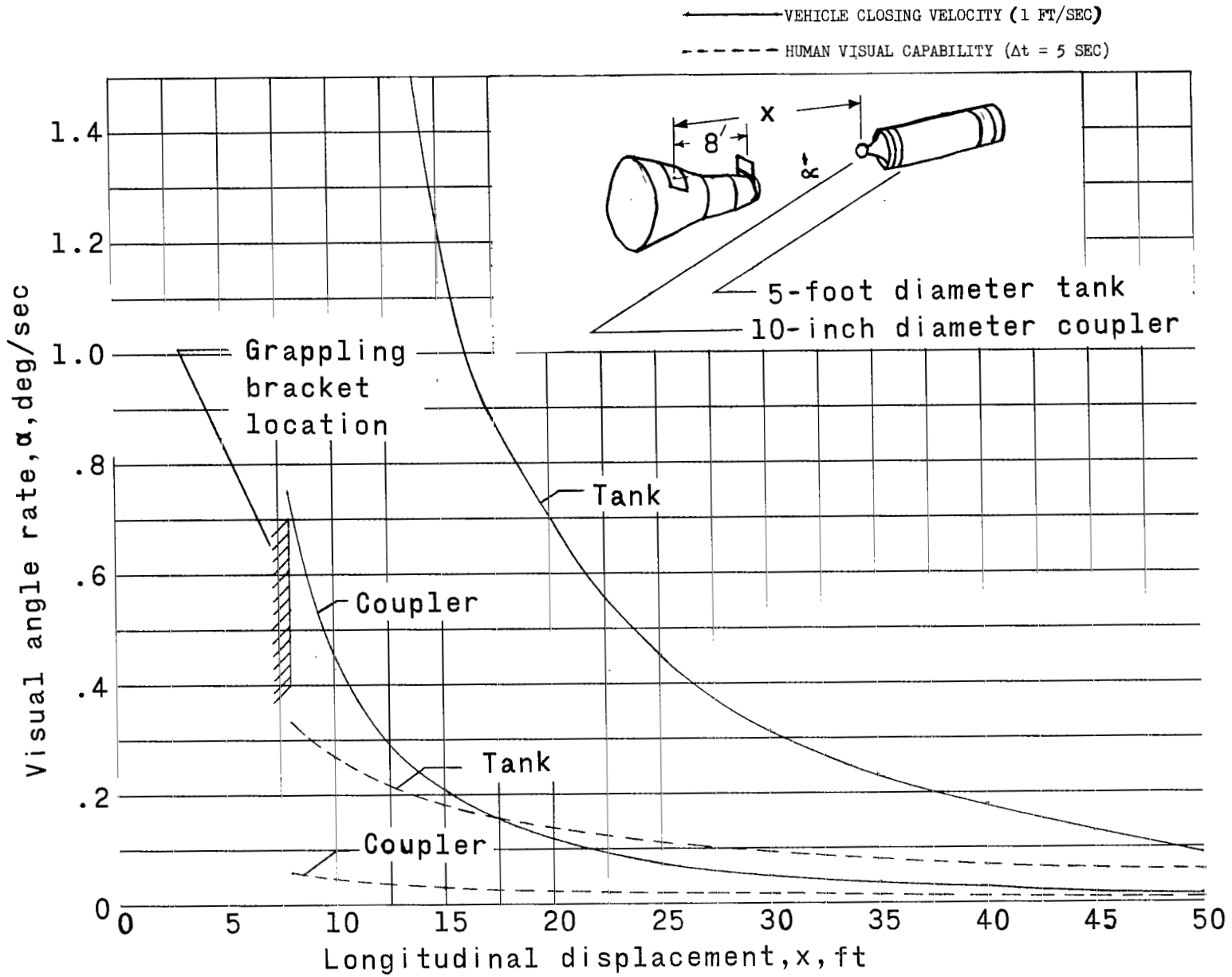

Figure 19.- Variation of the time rate of change of visual angle with distance for configuration of figure 1 for a longitudinal closing velocity of 1 ft/sec compared with the associated minimum detectable visual curves that were computed for an observation time of 5 seconds.

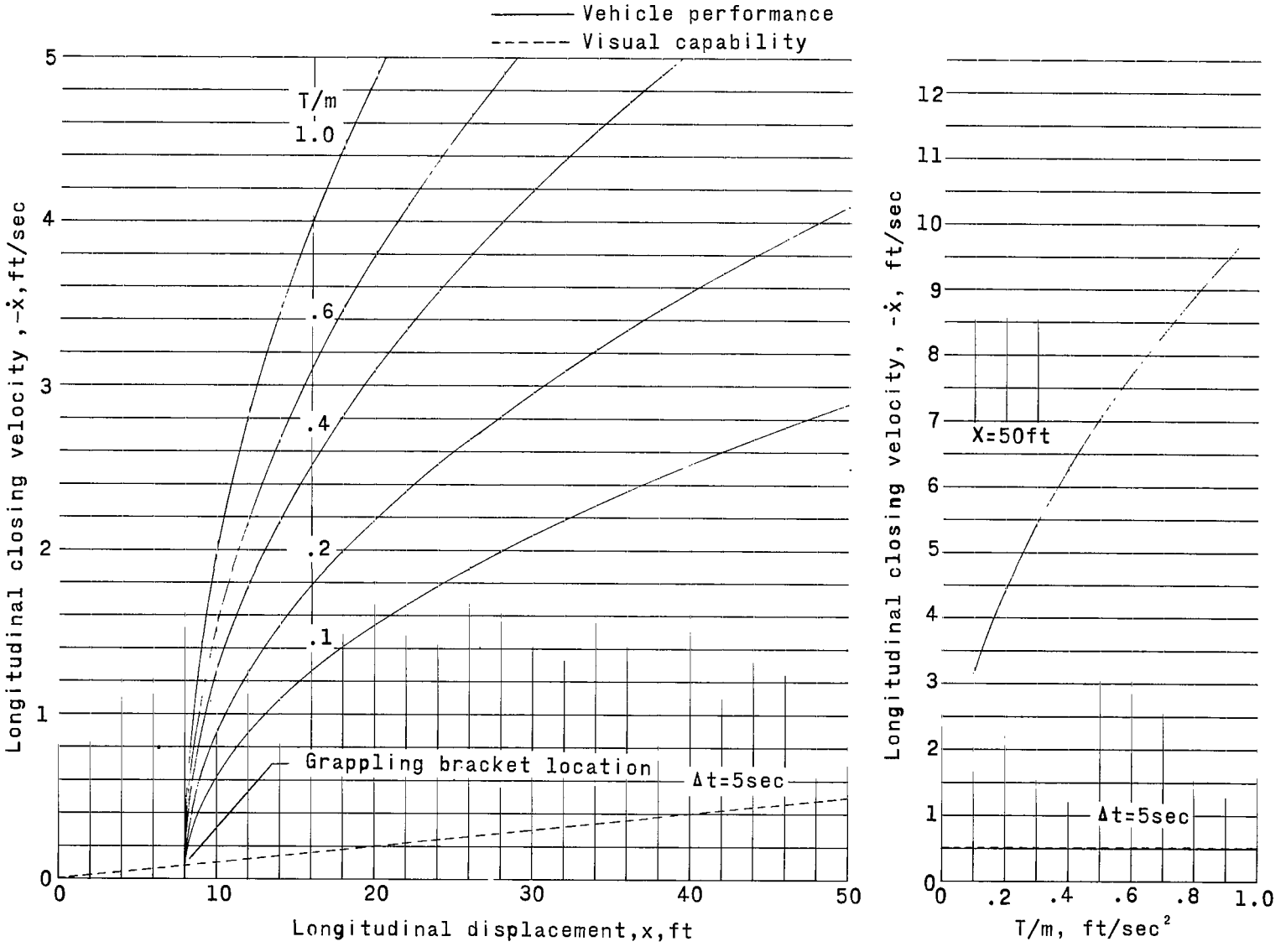

Figure 20.- Performance charts for displacements up to 50 feet showing human visual capability for one observation time as compared with the maximum vehicle velocity that constant thrust application can reduce to zero at the grappling bracket.

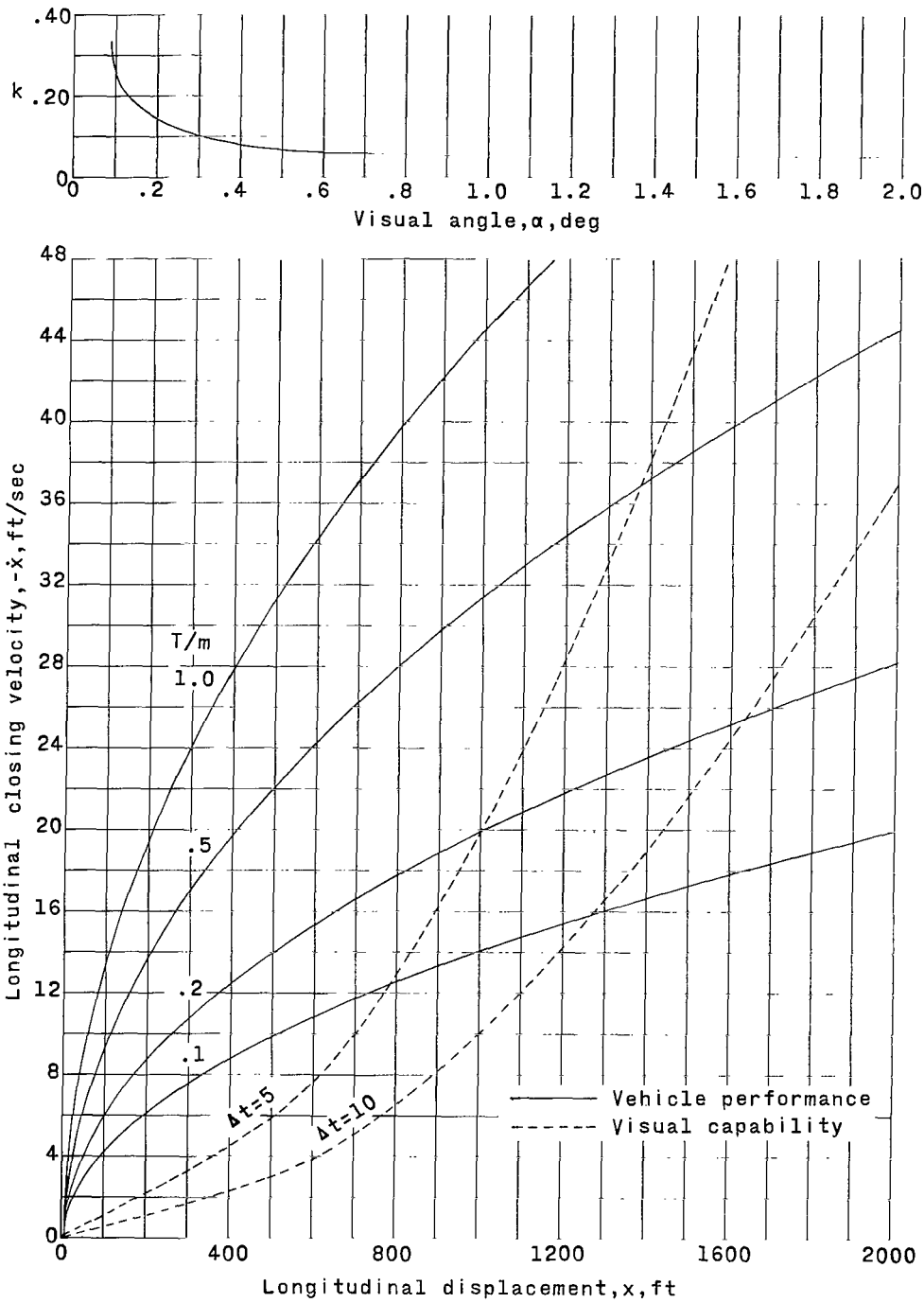

Figure 21.- Performance chart for large displacements illustrating the degradation in human visual capability for judging closing velocity with longitudinal displacement for a 5-foot-diameter vehicle for two observation times. Vehicle performance curves give maximum vehicle velocity that can be reduced to zero at grappling bracket for constant thrust application. (Visual capability curves utilize k against α curve as shown.)

NASA-Langley, 1964 L-3561